Acta Astronautica 219 (2024) 300–317

Contents lists available at ScienceDirect

Acta Astronautica

journal homepage: www.elsevier.com/locate/actaastro

Evaluation of the thermo-elastic response of space telescopes using uncertainty assessment

Uxia Garcia-Luis [a,*], Alejandro M. Gomez-San-Juan [a], Fermin Navarro-Medina [a], Alba Eva Peláez Santos [b], Pablo Gonzalez De Chaves Fernandez [c], Alfonso Ynigo-Rivera [c], Fernando Aguado-Agelet [d]

[a] atlanTTic, Universidade de Vigo, Escola de Enxeñaría Aeronáutica e do Espazo, Aerospace Technology Research Group, 32004, Ourense, Spain
[b] ESA-ESTEC, co ATG Europe BV, Keplerlaan 1, 2201AZ, Noordwijk, the Netherlands
[c] Instituto de Astrofísica de Canarias (IAC), c/Vía Láctea, s/n, 38200, La Laguna, Tenerife, Spain
[d] atlanTTic, Universidade de Vigo, Escola de Enxeñaría de Telecomunicación, Aerospace Technology Research Group, 36310, Vigo, Spain

ARTICLE INFO

Keywords:
Thermo-elastic
Space telescope
Earth observation
Uncertainty
Performance

ABSTRACT

The aerospace sector is evolving due to reduced launch costs and standardization of small satellite platforms. This research, aligned with European Guidelines for Thermo-Elastic Verification, addresses the pointing precision gap in small satellites by assessing space telescope performance using uncertainty propagation in thermo-elastic models. The methodology will be directly applied to an Earth observation space telescope, VINIS, currently under development by the Instituto de Astrofísica de Canarias (IAC). This procedure helps to identify key design elements impacting its functionality. Thirteen elements were identified as main contributors to the deformations in the optical bench. Due to the bench's crucial role in the telescope's performance, this paper also explores how results vary with different sandwich panel modelling techniques and the enhancements from design modifications. While the focus is on space telescopes, this approach has broader applicability to thermo-elastic analysis of various space instruments.

1. Introduction

1.1. Growth of the space telescopes missions and increasing relevance on performing thermo-elastic analyses

In recent years, there has been a remarkable increase in the use of space-based telescopes, emerging as essential tools for driving scientific progress [1]. The study and advancement of these cosmic observatories had an immense impact on humanity across several domains, serving as sources of invaluable information that profoundly benefits both the scientific community and society at large. One of the most important advantages of space telescopes lies in their capacity to investigate the cosmos beyond the constraints of the Earth's atmosphere. By deploying telescopes into orbit, astronomers are able to explore celestial objects with unprecedented precision and detail. This, in turn, has propelled our comprehension of the universe's origins and evolution to new levels. Furthermore, these space-based instruments are pivotal for Earth observation, delivering crucial data for applications ranging from disaster management to strategies addressing the pressing issue of climate change [2,3]. There is a rise in the number of space missions equipped with telescopes, including both those currently under development and those scheduled for launch by organizations such as the European Space Agency (ESA) in the upcoming years. This scenario highlights the shifting paradigm within the realm of space exploration and satellite deployment. Traditionally, mission design prioritized safety above everything else. However, there is a prevailing trend to assume higher risks in exchange for significantly reduced costs. This shift is particularly evident with the implementation of small satellite platforms, which have democratized access to space through lower launch costs and increased standardization [4].

Nevertheless, ensuring the precise pointing accuracy and stability of these space telescopes, especially for the smaller satellite platforms, presents a significant challenge [5]. As telescopes continue to enhance

* Corresponding author.
E-mail addresses: uxia.garcia.luis@uvigo.gal (U. Garcia-Luis), alejandromanuel.gomez@uvigo.gal (A.M. Gomez-San-Juan), fermin.navarro.medina@uvigo.gal (F. Navarro-Medina), albaeva.pelaezsantos@ext.esa.int (A.E. Peláez Santos), dechaves@iac.es (P. Gonzalez De Chaves Fernandez), alfonso.ynigo.rivera@iac.es (A. Ynigo-Rivera), faguado@uvigo.gal (F. Aguado-Agelet).

https://doi.org/10.1016/j.actaastro.2024.03.029
Received 1 November 2023; Received in revised form 12 March 2024; Accepted 14 March 2024
Available online 15 March 2024

Abbreviations

BEE	Back End Electronics
CTE	Coefficient of Thermal Expansion
CONOPS	Concept of Operations
DoF	Degrees of Freedom
ECSS	European Cooperation for Space Standardization
ESA	European Space Agency
FEM	Finite Element Model
FPA	Focal Plane Assembly
GMM	Geometrical Mathematical Model
GSA	Global Sensitivity Analysis
HST	Hubble Space Telescope
I-METER	Improvement Of Methodologies For Thermo-Elastic Predictions And Verification
IM	Influence Matrix
IP	Input Parameter
IAC	Instituto de Astrofísica de Canarias
JWST	James Webb Space Telescope
LoS	Line of Sight
MCRT	Monte Carlo Ray Tracing
MCS	Monte Carlo Simulations
OAT	One At a Time
PWT	Patch-Wise Temperature
PP	Performance Parameter
PLATO	PLAnetary Transits and Oscillations of stars
PDR	Preliminary Design Review
PAT	Prescribed Average Temperature
M1	Primary mirror
RSS	Root Sum Square
M2	Secondary mirror
SEA	Statistical Error Analysis
S	Structural Parameter
STOP	Structural-Thermal-Optical-Performance
TEV	Thermo-Elastic Verification
TGR	Thermal Geometrical-Radiative Parameter
TMM	Thermal Mathematical Model
TNR	Thermal Non-Radiative Parameter
TNRP	Thermal Non-Radiative PAT Parameter
TR	Thermal Radiative Parameter
TEDM	Thermo-Elastic Deformation Mechanisms
URQ	Univariate Uncertainty Quadrature

their optical capabilities, they become progressively more sensitive to deviations from the desired pointing attitude. Although some small satellite platforms have achieved impressive pointing stability, their performance has been till now insufficient for certain applications, including optical communications, astrophysics research, and precise Earth observation. Consequently, this technological gap needs to be bridged to allow these compact platforms reaching their full potential. To address this issue comprehensively, it is imperative to consider all the sources of error and disturbances contributing to the pointing error budget. Following the formal definitions provided in the ESA standards, known as the European Cooperation for Space Standardization (ECSS), these error sources can be categorized into four primary groups: bias, drifts, harmonics, and noise. Although high frequency vibrations also influence the satellite control system [6], this research focuses on developing a methodology for analysing quasi-stationary low-frequency disturbances associated with thermo-elastic deformations. This is because the slow nature of temperature variations that induce structural deformations which in turn cause optical performance errors and degradation [7,8]. The simulations predicting the thermo-elastic deformations are of immense importance since, once in orbit, detecting these disturbances is challenging.

1.2. Building upon the European guidelines: adapting the framework

Aware of these problems, ESA has recently published the first European Guidelines for Thermo-elastic Verification [9]. Their approach acknowledges the diverse nature of these problems, each presenting unique characteristics. Often, these distinctions are attributed to the innovative instruments implemented, suggesting that reliance on data from previous missions may not always be applicable. Consequently, the objective is not to offer a step-by-step guide for these analyses. Instead, the emphasis is on a methodology that facilitates the identification and mitigation of potential thermo-elastic issues by professionals developing such projects.

The methodology developed includes a systematic numerical process, aimed at verifying the system's compliance with the requirements. This process consists of four steps: (i) identification, (ii) modelling, (iii) classification and (iv) final performance compliance verification. For this methodology to be applicable to any thermo-elastic study, the guidelines need to introduce several definitions. The most important are the concept of "performance parameter" and "deformation mechanisms". The first relates to the quantification of the environmental effects on instrument performance, while the second is associated with structural deformations potentially compromising performance [9,10]. These guidelines employ the Influence Matrix (IM) approach, which has been previously used by Thales Alenia Space for the Improvement of Methodologies For Thermo-Elastic Predictions And Verification (I-METER) studies [11], demonstrating the validity of the methodology.

Researchers of the present study, however, focus their attention on the application of a methodology for the thermo-elastic performance evaluation of space telescopes. The procedure implemented in this research article is based on the recommendations provided in Ref. [9], and emphasizes the use of performance parameters to quantify the system response. While the heart of this approach is derived from these guidelines, certain aspects have been adapted based on methodologies applied to previous thermal studies developed by the authors of this paper [12–16], which have proven to be efficient. The primary aim of this work is to evaluate the feasibility of extending a procedure based on uncertainty quantification to the thermo-elastic evaluation.

1.3. Uncertainty-based methodologies for predicting system performance

Space engineering demands rigorous error control due to the strict weight, space, and cost constraints. Applying corrections once the satellite is in orbit is seldom possible; thus, minimizing errors during design and production becomes vital. One approach to achieve this objective is by conducting an exhaustive uncertainty assessment and impact analysis. Complex systems rely on mathematical models for performing trade-offs, design refinements, supporting mission compliance verification. Model validation is essential, ensuring they accurately represent the system and efficiently predict its behaviour [17]. Model accuracy is influenced by uncertainties in parameter values, representation limitations, and the impracticality of running every possible configuration. Parameter values are often ideal or from limited lab tests, which may not align with the actual system. Moreover, engineers typically introduce effective parameters due to complexity and hardware interactions, which are hard to replicate, especially in complex systems. Therefore, model outcomes have inherent uncertainties, impacting design decisions, cost, and performance. Currently, there is no standardized method for computing uncertainties in space thermo-elastic analysis. Nevertheless, approaches as application of pre-established margins, One At a Time (OAT), and stochastic methods are common [18].

The primary and widely used approach involves applying pre-established margins, usually derived from comparisons between model results and flight data [19,20]. However, this method lacks uncertainty propagation and, is trying to cover the uncertainty with safety factors to add conservatism, can sometimes give a false sense of safety [21–23].

OAT methods, such as Statistical Error Analysis (SEA) [24], initiated in 1953, propagate uncertainties via sensitivity coefficients. Specifically, the SEA method computes final uncertainty from Root Sum Square (RSS) of contributions, correlating parameter effects with performance. This simplicity facilitates initial uncertainty exploration but overlooks parameter interactions. It is aligned with ESA procedures recommended in thermal analysis standards, but recent standards lack specific uncertainty calculation methods [13,25–27]. Finally, this analysis identifies, classifies, models, and propagates uncertainties, enhancing system understanding, performance impact, and compliance with key parameters.

Advances in computing capabilities have paved the way for the use of stochastic techniques in uncertainty analysis, such as Monte Carlo Simulations (MCS) [28–31]. These methods, while relying on some simplifications, require more extensive resources and preparation. In contrast, the 2k+1 Rosenblueth method [32], which is a point estimate approach, may prove inadequate when dealing with substantial input dispersion. Univariate Uncertainty Quadrature (URQ) emerges as an alternative, offering both efficiency and precision. Notably, URQ does not rely on derivatives, rendering it especially advantageous in the context of gradient-based optimization [33]. These computational methods hold immense potential across diverse applications within the field of space projects. Incorporating a thorough assessment of probability distributions pertaining to input parameters is of huge relevance. Valuable data sources, as listed in Refs. [34–40], serve as critical references to this end. It is frequently observed that, in the absence of data, the default assumption of either uniform or normal distributions prevails, underscoring the limitations of our knowledge concerning parameter distributions.

1.4. Uncertainty analysis applied to space telescopes

With the progress of technology, the resolution requirements placed upon telescopes have increased. To support these increasing needs, it is required to perform a comprehensive analysis evaluating the thermo-elastic effects and Structural-Thermal-Optical Performance (STOP) efficiency, addressing factors contributing to optical performance degradation [7]. The implications of thermo-elastic effects on space telescopes have been widely recognized [41], as evidenced by their decisive role in missions like PLATO, whose 34 telescopes must be kept aligned, and where stability has proven to be a challenge [42]. The relevance of these factors is further accentuated by in-orbit issues that have affected missions such as Herschel and Hubble Space Telescope (HST), emphasizing the relevance of thermo-elastic and STOP analysis [43,44].

The design of telescopes has emerged as a critical juncture where the mitigation of thermal and mechanical deformations is mandatory to ensuring successful optical performance [45–47]. The literature reveals a scarcity of published papers focused on telescope performance evaluation through uncertainty analysis [48]. Nevertheless, there have been noteworthy endeavours in this direction, including a study developed by authors of this paper to assess the Earth observation telescope VINIS [15]. Another study which applied multifid uncertainty quantification techniques to evaluate the performance of the James Webb Space Telescope (JWST) under the influence of thermal loads is [49]. These multifid approaches have demonstrated their potential in rendering uncertainty quantification and optimization viable across a spectrum of applications. Global Sensitivity Analysis (GSA) has emerged as a tool for quantifying the sensitivity of performance parameters within numerical models to their underlying inputs [50]. Moreover, the cutting-edge introduction of a novel multifid estimator designed to compute the global sensitivity has increased the efficiency and streamlined the analysis, as it promises to significantly reduce computational time [49].

1.5. VINIS telescope

This paper implements the thermo-elastic evaluation methodology to VINIS, an innovative, cost-effective telescope currently under development by *Instituto de Astrofísica de Canarias* (IAC). Its platform falls under the small satellite category, as the telescope weights around 12 kg. The maximum dimensions of the complete telescope assembly are 650 × 480 × 450 mm. VINIS is designed to capture high-resolution images with a resolution of one pixel per 5 m. Its capabilities make it particularly effective for capturing images of urgent global events. These scenarios include natural disasters such as earthquakes, floods, and wildfires, but also instances related to global warming or monitoring of oil spills in oceans.

VINIS has just undergone the Preliminary Design Review (PDR). This is well aligned with one of the potential benefits of this methodology, which is to showcase the potential in detecting issues from preliminary designs. As depicted in Fig. 1, the telescope's design employs a Cassegrain configuration. Its operation involves incident rays reflecting on the primary mirror (M1) and then on the secondary one (M2), directing them toward the focal plane, which is situated slightly behind the primary mirror. Here, a set of lenses in an optical vehicle correct aberrations. Behind them lies the Focal Plane Assembly (FPA) with the detector.

The telescope was designed based on the principles of iso-thermal and iso-static mounting. To implement the iso-thermal design concept, the engineers responsible for the optical design proposed an aluminium structure surrounding the M1 and M2 mirrors, which are also metallic, providing thermal stability and preventing optical performance degradation under all temperature conditions.

To ensure an iso-static mounting, VINIS is structurally supported by three titanium bipods. These bipods are attached to an optical bench comprised of a sandwich panel, orthogonal to the observation direction. The sandwich panel supporting the telescope assembly also has the main baffle and an electronic box attached, with the latter located on the opposite side of the telescope mounting. This optical bench is assembled with another sandwich panel mounted at 90° along the telescope axis, which also supports part of the central baffle structure with the help of a small sandwich panel support. All sandwich panels are joined together via carbon-fibre brackets. In conclusion, this design aims to offer a cost-effective solution with exceptional image resolution capabilities, making it well-suited for capturing global images during critical situations.

There are some preliminary findings about the thermo-elastic analysis of VINIS telescope in Ref. [15]. From this initial exploration, it became evident that the modelling of sandwich panels from the optical benches were essential in determining the final optical performance. Consequently, the future research lines that emerged from that study were aligned with the examination of the sensitivity of the results to the implementation of 2D or 3D formulation of the sandwich panels. Further, it would be interesting to introduce modifications to the original design based on these findings. This would offer a robust evaluation of the methodology's efficiency and its potential to address thermo-elastic challenges.

1.6. Article outline

This paper is organized as follows. The (i) Introduction highlights the rising number of space telescope missions and underscores the significance of thermo-elastic analyses, especially for high-precision pointing systems. It also evaluates the reliance on uncertainty-based methods for predicting system performance. The (ii) Objectives section sets out our primary goal: to showcase the efficiency of uncertainty methodologies in this domain and to assess how different modelling techniques impact sandwich panels response. The (iii) Methodology section provides a thorough breakdown of the thermo-elastic analysis process, the principles of the uncertainty-based approach, and an overview of the key parameters. In the (iv) Numerical Models section, the thermal and

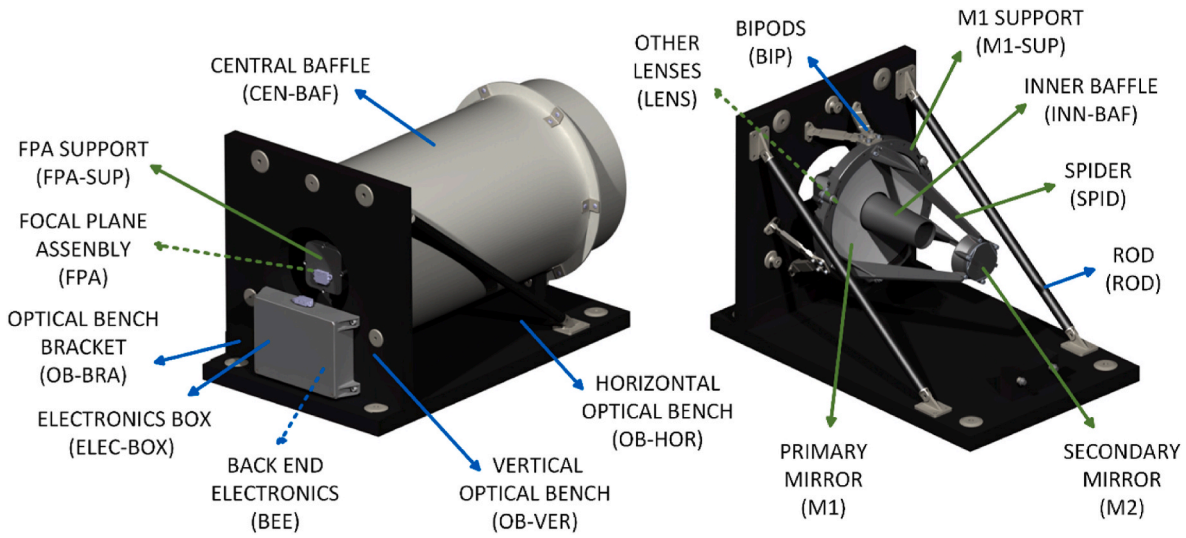

Fig. 1. VINIS telescope assembly components indicated with blue arrows and main telescope train in green. Hidden components marked with dotted arrows. Nomenclature employed in the paper within parenthesis. (For interpretation of the references to colour in this figure legend, the reader is referred to the Web version of this article.)

structural models' formulation and parametrization have been presented. The (v) Results section emphasizes the thermo-elastic design elements that most influence telescope performance. Lastly, the (vi) Discussion and (vii) Future lines sections capture the study's main findings while suggesting potential fields for further refinement and exploration.

2. Objectives

The main objective of this paper is to further evaluate the performance of a novel analysis methodology based on uncertainties to identify and quantify degradations in space telescopes due to thermo-elastic effects. It also aims at collecting the best practices in an analysis procedure, for optimal evaluation of thermo-elastic deformations.

The secondary objectives were identified based on the preliminary findings from Ref. [15]. Consequently, the study evaluates the impact of using either a 2D or 3D representation of the optical benches' sandwich panels in the analysis. Additionally, the study seeks to propose design changes based on uncertainties results, specifically to meet strict the performance requirements. These objectives are set to provide a deeper understanding of how the modelling choices influence the overall findings.

Moreover, the developments made shall be compatible with the employment of the software preferred in most ESA-led missions: ESATAN, SINAS, and NASTRAN software (for thermal analysis, temperature mapping, and structural analysis, respectively). Regardless of the specific tools mentioned, the analytical process shall be seamlessly adapted and applied to alternative software platforms.

3. Methodology

3.1. Detailed procedure for developing thermo-elastic analysis

In most spacecraft projects thermal and structural analysis are self-contained and executed in isolation from other disciplines. However, one of the primary challenges in conducting thermo-elastic stems for its intrinsic multidisciplinary nature. There is a need for involving a variety of fields to evaluate the thermo-elastic performance of an instrument, which, in the case of space telescopes, includes at least thermal, structures, optics, and systems engineering disciplines. For the sake of efficient planning, coordination, data transfer and communication it is recommended to form at the beginning of the project a dedicated team with specialists from the mentioned disciplines specifically for the complete thermo-elastic verification process [9]. To coordinate all of them, it is essential to understand from outset the different steps to be carried out, as well as their interrelation.

The literature review revealed that there are several sources providing isolated advice on how to develop thermo-elastic analysis of space telescopes. Here, the guidelines made a comprehensive compilation of all these suggestions, easing the process. However, sometimes given the numerous interdependencies between the analyses, applying all the recommended processes in the most efficient manner was the result of multiple iterations. For this reason, the establishment of an analytical procedure is of great interest. Authors of this paper compile in Fig. 2 a six-phase nominal thermo-elastic analysis procedure that outlines the steps to be taken, indicating their sequence and interrelation. It is relevant to mention this procedure is specified for the use of ESATAN, SINAS and NASTRAN software — chosen due to their prevalent usage in ESA-led missions. In case other software is employed, there are steps which may be subjected to some changes. As example, the employment of the Prescribed Average Temperature (PAT) method for temperature mapping (implemented in SINAS) [7,51,52], requires the creation of a structural conductive numerical model. Conversely, when methods like Patch-Wise Temperature (PWT) [7] are employed, phase 4.3 could be omitted.

The process for nominal thermo-elastic analysis begins with Phase 0, where the requirements and scope of the study are identified, based on the performance parameters of the instrument being analysed. This first step ensures that all parties share a unified understanding of the mission's objectives. With this overview, phase 1 accentuates the importance of building consensus around the modelling approach. In this context, the multidisciplinary TEV (Thermo-Elastic Verification) team, primarily comprising thermal and structural engineers and guided by optical engineers, determine the most effective representation of the instrument's component based on previous experience and initial understanding of the behaviour of the structure. Therefore, the primary goals for building the model shall be to (i) accurately represent all Thermo-Elastic Deformation Mechanisms (TEDM), (ii) to guarantee that every TEDM aligns with a model parameter suitable for an uncertainty analysis, and (iii) to build a model as simple as possible that meets the first two objectives.

Progressing to phase 2, the emphasis on establishing agreement on the level of idealization of the actual often detailed geometry of the structure for implementation in both the thermal and structural model.

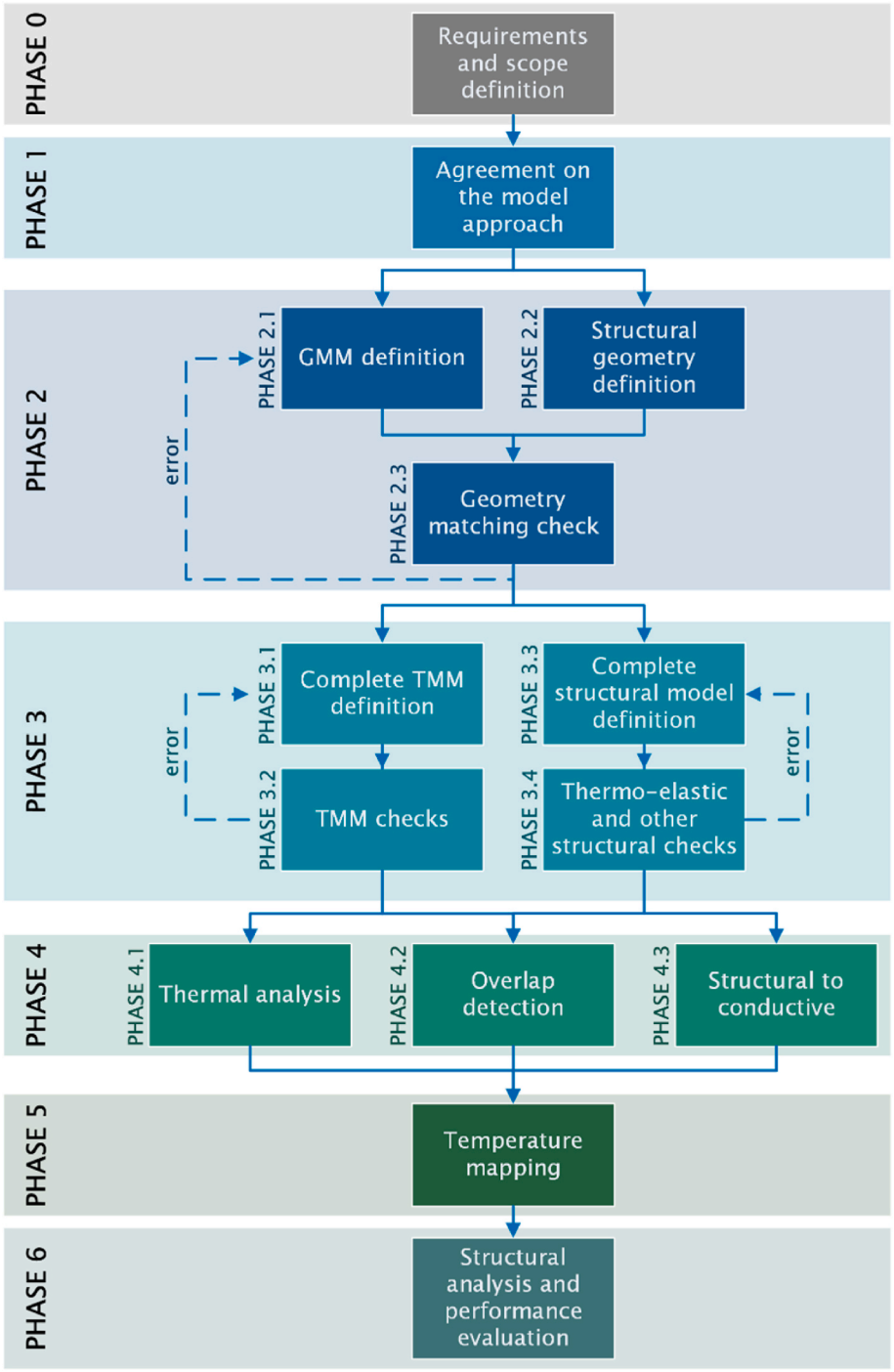

Fig. 2. Procedure proposed to perform a nominal thermo-elastic analysis.

This step is essential for streamlined temperature mapping in the following phases. With these geometries set, phase 3 shifts the focus to the detailed development of the thermal and structural models. While these models can be concurrently developed, it is important to ensure that data (e.g., material's properties) is gathered from the same sources of information.

Phase 4 entails the compilation of essential inputs necessary for executing the temperature mapping. This process involves three simultaneous tasks: computing the temperature distributions through thermal analysis, performing the overlap detection between the thermal and structural meshes, and adapting the structural model to its conductive variant. This conversion accounts for thermal linkages, ensuring that the upcoming temperature mapping is executed with precision. Phase 5 performs the temperature mapping, based on the three inputs coming from the previous phase. Finally, phase 6, involves executing the structural analysis and obtaining the performance parameter's results, either directly from the deformations or through subsequent computations. Phases 4 to 6 are grouped as they encompass the processes that must be implemented for the application of the uncertainty methodology.

3.2. *Implementation of the thermo-elastic uncertainty analysis*

Implementation of the thermo-elastic uncertainty analysis, as

highlighted in the introduction of this paper, deviates slightly from the nominal procedure as presented in the European guidelines [9]. This deviation is motivated by the requirement of assessing the efficiency of employing an uncertainty methodology for performance evaluations. While this methodology has proven useful in the development of thermal analyses [13], this research aims to determine its applicability and effectiveness in the thermo-elastic domain.

An important requirement to apply the uncertainty methodology, is that both the thermal and structural models are set up parametrically. This approach facilitates the assessment of a large number of parameters in a simple manner. An essential component for this is having an automated analysis process, which in this case was implemented using Python. One of the advantages of this method is that it simplifies the phase (i) identification. Furthermore, it might help identify critical parameters that were not initially considered. However, it remains crucial for the engineers involved in conducting the analysis to accurately describe and model the thermo-elastic deformation mechanisms, and to be able to evaluate the outputs of the analysis correctly.

The parameter identification between the guidelines and this method only differentiates in the selection of the input parameters (or "features"). Whereas the European Guidelines [9] identifies the thermal, structural, and thermo-mechanical groups, the uncertainty-based methodology further differentiates the thermal parameter into three categories, TGR, TR, and TC, which are defined on Table 1. This is useful mainly when implementing the methodology since, due to the intrinsic characteristics of the ESATAN program, the parameters related to thermal analysis can affect three, two, or a single phase of the software run. The definitions of all the parameters involved in this analysis, is gathered in Table 1.

In Fig. 3, there is a schematic representation of the complete process adopted for uncertainty quantification. This process is exclusively associated with phases 4 through 6 (Fig. 2). Like the European guidelines [9], the methodology presented in this paper is designed to be applied once the instrument's preliminary configuration is set. While the methodology offers the ability to automate and modify parameters, any significant modification of the design (e.g., geometry), will require repeating phases 1 to 3, needed to capture the effects of the design changes in the process (see Fig. 4).

Furthermore, it is important to emphasize that the process illustrated in Fig. 3's diagram corresponds solely with phases of (iii) classification and (iv) final performance compliance verification, from Ref. [9]. The intention of the classification step is to determine which parts of the structure are providing the highest contribution to the response of the performance parameters. Uncertainties in those parts are most relevant to investigate. However, guidelines [9] lack of a comprehensive advice on specific methods for evaluating these uncertainties. This research article aims to address this gap, offering a method which complement the guidelines by focusing on uncertainty analysis of the design elements which most contribute to the degradation of the performance parameters.

After performing the review on the uncertainty methodologies for predicting system performances, the SEA method was selected as the uncertainty propagation technique, as it offers a compromise between the quality of the information obtained and computational effort. While the method itself is not new, its use in evaluating space telescope performance is innovative.

Even though this method has several advantages, it also has some limitations. One limitation is its failure to account for interactions between parameters. Additionally, it makes certain simplifying assumptions which are not always met: (i) linearity of the models, (ii) statistical independence, and (iii) normal gaussian distribution of all the parameters under study. Despite these limitations, the method still provides valuable insights into which parameters most significantly affect the thermo-elastic response. Although there may be some errors in numerical calculations, the results offer a qualitatively accurate approximation, making it suitable for implementation even in the very early design phases.

The method consists of obtaining the derivatives with respect to the parameters $\partial P_i/\partial x_k$ (sensitivity coefficients) and calculating the associated uncertainties by multiplying these by the uncertainty values w_{Xk} of the x_k parameters for a given confidence level. The value of the performance parameters (P_i) can be defined as:

$$P_i = P_i(x_1, x_2, \ldots, x_k)$$

Given the uncertainty values w_{kx} for the x_k parameters for a defined level of confidence σ_n, the uncertainty of the performance parameters for that same level of confidence can be expressed as:

$$w_{P_i} = \left[\left(\frac{\partial P(x_1, \ldots, x_k)}{\partial x_1} w_{x1} \right)^2 + \ldots + \left(\frac{\partial P(x_1, \ldots, x_k)}{\partial x_k} w_{xk} \right)^2 \right]^{1/2}$$

Sensitivity coefficients are calculated numerically by determining the deviations in performance parameters ($P + \Delta P$) resulting from slight modifications to the nominal values of the input parameters ($x + \Delta x$), as illustrated in Fig. 3. In this analysis, it was employed as Δx a 1% deviation from the nominal value. As the final SEA uncertainty is derived from the root mean square of the different contributions, the final uncertainty for each performance parameter can be easily related to the contributions of the input parameters.

Following the European guidelines [9], a preliminary study of the potential thermo-elastic deformation mechanisms was conducted. This evaluation involved collaboration between performance and thermal-structural engineering teams. Their joint efforts ensured that the model captured these deformations. The initial step was identifying the parameters that indicate the instrument's performance. Key indicators for its proper functioning include (i) the relative alignment

Table 1
Definitions of the uncertainty methodology implementation.

Type	Name	Abbreviation	Definition
General process	Performance Parameter	PP	An individual or combined thermo-elastic output that is pre-identified to measure the thermo-elastic design's performance. If its metrics are within the performance requirements, the instrument's performance is correct.
General process	Input Parameter	IP	Any potential feature of the physical or mathematical model that has potential to influence the thermo-elastic response.
Input parameter	Thermal Geometrical-Radiative	TGR	Characteristics that influence the instrument's response via the Geometrical Mathematical Model (GMM). Their impact is evaluated through the full analysis cycle.
Input parameter	Thermal Radiative	TR	Parameters from the space environment. To assess their impact, almost the entire thermo-elastic review needs to be revisited, beginning with the radiative case.
Input parameter	Thermal Non-Radiative	TNR	Factors influencing only the thermal study's final phase, the Thermal Mathematical Model (TMM), e.g., internal heat dissipation. Only the latter part of the thermal study, mapping, and structural analysis is required.
Input parameter	Thermal Non-Radiative PAT	TNRP	Thermal elements affecting all stages: thermal analysis, temperature mapping, and structural analysis. This is due to employing the PAT technique for temperature mapping. If a different method is applied, some factors might only influence the thermal analysis.
Input parameter	Structural	S	Structural element, that influence only the last part of the analysis process. The standard temperature field supplied by SINAS can be used to directly conduct the structural study.

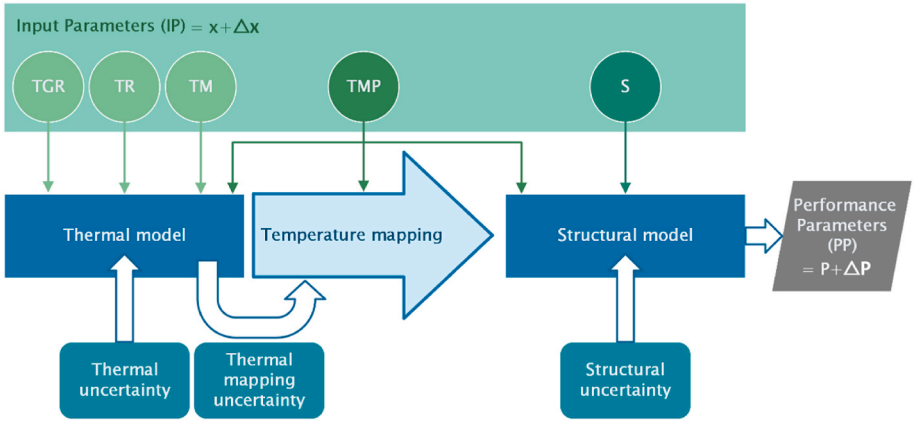

Fig. 3. Diagram of the methodology for thermo-elastic uncertainty assessment (see Table 1 for acronyms).

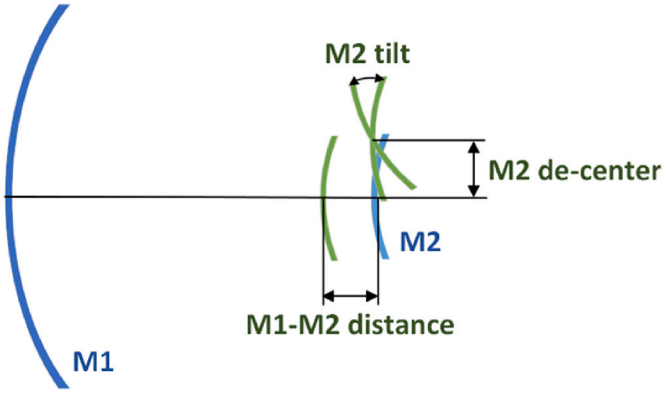

Fig. 4. Possible misalignments between the two mirrors (in blue), forming the three performance parameters (in green). Diagram modified based on: [53]. (For interpretation of the references to colour in this figure legend, the reader is referred to the Web version of this article.)

between mirrors (M2 tilt), (ii) in-plane displacement of the M2 mirror (M2 de-center), and (iii) the distance between mirrors (M1-M2 distance). The acceptable limit values for the telescope's performance were also determined.

Table 2 shows the parameters evaluated for the thermo-elastic model, including their type and associated uncertainties. In total 148 are considered. The uncertainty associated to thermal parameters was determined using Table.6–1 and 6–2 from Ref. [54], while the uncertainty for structural parameters was based on experience. Uncertainties for properties like thermal conductivity (k) and Young's Modulus (E) vary by material type: 10% for isotropic, 20% for orthotropic, and 30% for anisotropic materials, when their effective properties are used. Moreover, the uncertainty in calculating sandwich stiffness differs between 2D (50%) and 3D (30%) formulations.

4. Numerical models

4.1. Thermal model

Besides developing the thermo-elastic analysis of VINIS, authors of this paper also conducted in parallel a thermal analysis for defining a passive protection for its platform. These activities proved to be very useful in understanding the Concept of Operations (CONOPS) and, consequently, the most demanding thermal environment conditions. Fig. 5 presents the geometrical thermal model with schematic representation of the primary components in a preliminary conceptual design of the VINIS platform.

Table 2
Main Input Parameters categories for thermo-elastic analysis, and its standard deviation for the analysis of the VINIS telescope [16].

Input Parameter (IP)	Symbol	Type	Uncertainty of the nominal value (2σ)	Number of parameters analysed
IR emissivity	ε	TGR	3%	4
Solar absorptance	α	TGR	3%	4
Solar constant	J_S	TR	0.36 %	1
Earth albedo	a	TR	0.33%	1
Earth flux with Black Body Temperature	J_P	TR	25.5%	1
Heat dissipation	Q_i	TNR	20%	2
MLI efficiency	MLI_{eff}	TNR	50%	1
Conductive coupling	GL	TNRP	100%	1
Contact resistance	h	TNRP	100%	6
Thermal conductivity	k	TNRP	10–30%	9
Young Modulus	E	S	10–30%	4
CTE	CTE	S	10%	6
Joint axial stiffness	k_{j-ax}	S	50%	25
Joint bending stiffness	k_{j-be}	S	50%	25
Joint shear stiffness	k_{j-sh}	S	50%	50
Sandwich in-plane stiffness	k_{s-ip}	S	30–50%	2
Sandwich bending stiffness	k_{s-be}	S	30–50%	2
Sandwich shear stiffness	k_{s-sh}	S	30–50%	2
Sandwich out-of-plane stiffness	k_{s-oop}	S	30–50%	2

Thermo-elastic analysis uses detailed Thermal and Geometric Mathematical Models (TMMs and GMMs) to represent temperature maps [27]. These models differ from standard thermal models, as they incorporate more detailed geometry to capture temperature changes in joints that can influence the state of constraint. Regular, thermal control models, developed for thermal control purposes, often overlook these details [7,55].

The VINIS geometric model (GMM, illustrated in Fig. 6) has the main parts divided into five modules: telescope assembly (orange), bipods (purple), electronic box (green), optical benches (blue), and baffle (grey). The radiative calculations were conducted using the Monte Carlo Ray Tracing (MCRT) method. Settings for the radiative calculations were determined based on sensitivity tests to ensure accurate temperature readings.

The TMM for VINIS builds on the GMM and incorporates both conductive and radiative boundaries. Radiative exchange factors and

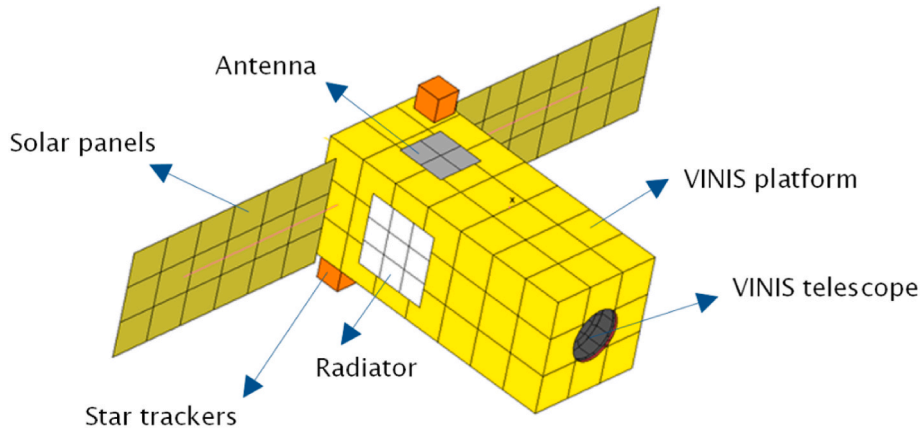

Fig. 5. VINIS' platform thermal model, which includes an MLI passive protection.

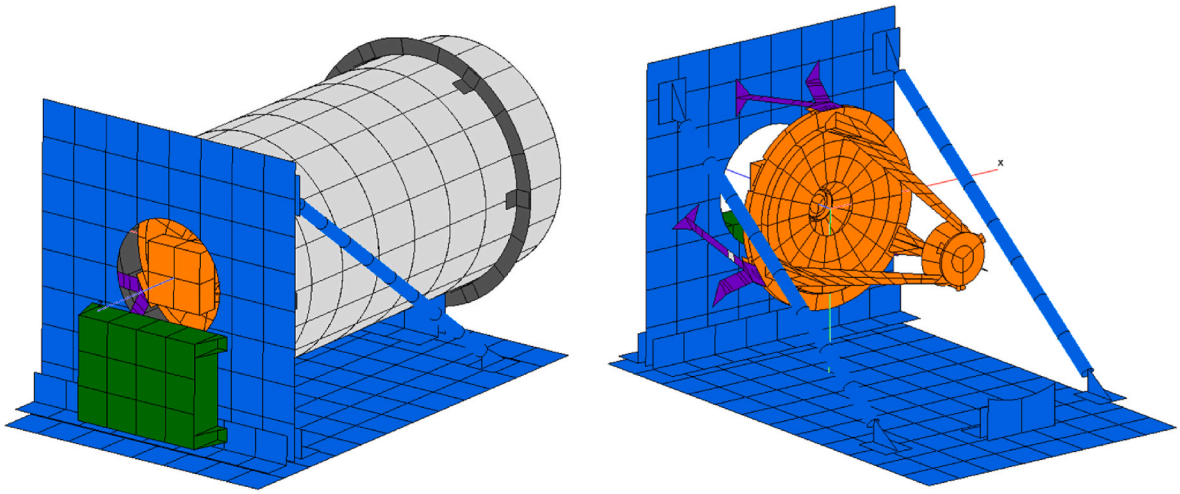

Fig. 6. VINIS's GMM in ESATAN.

some conductive couplings are calculated with ESATAN software, while others are analytically determined based on the mechanical contact. The model also includes power dissipating equipment, external loads like solar and Earth infrared, and deep space as boundary conditions. The TMM also accounts for the through-thickness thermal gradient on the optical bench's sandwich panels. This involves employing an effective conductance derived from the panel's material and thickness.

Parametrization for TGR and TR parameters involved modifying the ESATAN geometry and radiative files for each run. Conversely, TNR and TNRP parameters were centralized into a single text file, which was used as input for the thermal analysis case. This approach allowed for all variables to be linked to TNR and TNRP, enabling simultaneous adjustments to all related elements through changes made to just the TNR or TNRP values in this input file.

4.2. Finite element model (FEM)

The VINIS FEM was developed using the same CAD as for the GMM and TMM. To build a FEM, it is necessary to balance between detail and simplicity [56]. The model should precisely represent TEDM and be parametrized to characterize all TEDM aspects of the TNRP and S parameters listed in Table 2. For VINIS, the model was built using NASTRAN. Main structural components were modelled by CQUAD4 and CTRIA3 shell elements, including bipods, with struts represented by 1D CBAR elements.

Previous studies highlighted [15] that the optical bench and the deformations resulting from the dissipation from the electronics box (situated behind the vertical optical bench), play a significant role in degrading optical performance. This prompted a deeper examination in this study of how sandwich panels are modelled, resulting in the development of two analysis scenarios.

- **Configuration A**. 2D equivalent properties for the representation of the sandwich panel (PSHELL and MAT1), considering the uniform temperatures over the sandwich cross-section, as the average temperature of both sides (TEMP).
- **Configuration B**. An in-depth model of the sandwich panel, specifying the laminate at the top and bottom skins (PCOMP and MAT8, 2D) represented through CQUAD/CTRIA elements, and the honeycomb's equivalent properties (PSOLID and MAT9, 3D) represented through CHEX elements. This approach introduces several GRIDs through the thickness of the sandwich allowing to simulate temperature variation through the cross-section of the sandwich.

The transverse temperature gradient is consistently computed using interpolation with SINAS. Having three solid elements across the sandwich thickness allows for capturing transient effects in the form of nonlinear temperature distribution along the thickness coordinate [7]. For the honeycomb's 3D representation, was relied on the property data provided by the manufacturer (HexWeb).

In the case of the 2D approach, the PSHELL card enables the definition of equivalent properties for membrane, bending, and shear.

- In-plane loads on the sandwich panel are mostly handled by the skins, represented by MID1 (in this context, carbon fibre) with T_s denoting the total thickness of the two skins.
- Bending loads are supported again by the skins. Here, MID2 is associated with the skin material, while $12I/T_s^3$ represents the inertia of a plate (as depicted in the MSC Nastran Reference Guide), with $I = T_s T_c^2/4$ for $T_c \gg T_s$, where T_c is the core thickness.
- The honeycomb core (made of aluminium) is responsible for managing shear loads, referenced by MID3.

The interconnections between parts are represented by zero-length CBUSH elements linked by Rigid Body Elements, type 2 (RBE2). These embody the joint stiffness in the relevant Degrees of Freedom (DoF). Each RBE2 definition incorporates the Coefficient of Thermal Expansion (CTE) of the part it represents. Fig. 7 provides a closer look at these FEM models.

Due to some changes in the definition of the thermal and structural numerical models, the results from the previous paper [15] are correspondingly revised. Although the modifications are small, it is advised to establish all comparisons with the updated version of the VINIS model.

In addition to the initial two scenarios, a third variant, "**Configuration C**″, incorporates design modifications to the telescope based on preliminary insights. The preliminary uncertainty analysis performed to the telescope assembly [15] revealed that the parameters associate to sandwich panel stiffness do greatly contribute to loss of performance. Therefore, trying to reduce sandwich bending might be a way to improve performance of the telescope. Therefore, the authors of this paper decided to study a design change to try to meet all thermo-elastic requirements by fine-tuning the in-plane stiffness (along the direction coincident with the optical axis) of the connection between the rods and the horizontal optical bench. Physically, this would be implemented by installing a calibrated spring-like device. One of the two connections is highlighted in green in Fig. 7. The results will determine if these changes that were promoted by using the uncertainty methodology enhance the telescope's performance. This modification will affect the stiffness of some parts of the structure, and therefore it should be assessed if this loss of rigidity can be problematic with other structural requirements, such as the minimum natural frequency or the strength of the structure.

Material properties in the FEM model were directly implemented in a parametric way, with the CTE adjusted using the automation code which was developed for material and RBE2 definitions. The parametrization of joints was implemented via the PBUSH entry, linked to the CBUSH element that connects each RBE2 pair. It is important to carefully define the CBUSH coordinate system, to ensure that axial response aligns with stiffness in direction 1, shear in directions 2 and 3, and bending in directions 5 and 6. In this way, it is easier to consistently modify each joint stiffness.

For the 2D sandwich stiffness parametrization, the PSHELL implementation was employed. Despite MID1 and MID2 typically refer to the same material, they were duplicated to distinguish between in-plane and bending responses. The Young Modulus was modified accordingly, proportional to the in-plane ($k_{s-ip} = ET_s/(1-\nu^2)$) and bending ($k_{s-be} = EI/(1-\nu^2)$) stiffness of a plate. In the 3D formulation, the Young Modulus was similarly altered, with the PSHELL and MAT2 equivalence computed in accordance with the PCOMP and MAT8 formulation, considering Classical Lamination Theory for sandwich stiffness parametrization.

5. Results

5.1. Worst thermo-elastic scenario selection

The first step on performing the analysis, is to identify the most demanding thermo-elastic scenario. For this purpose, it is crucial to make the evaluation based on performance parameters, not just thermal outcomes. "Configuration B″ FEM nominal performance was monitored across Cold Operational Case (COC), Hot Operational Case (HOC), and Consecutive Imaging Case (CIC) scenarios, to identify the worst thermo-elastic conditions. Fig. 8 reveals that the M2 de-center is only parameter not meeting requirements. The worst-case scenario was thus determined when M2 de-center reaches its maximum. Nevertheless, as the performance parameters do not undergo any significant modification throughout the entire orbit, this criterion was combined with the identification in which moment thermal gradients are higher.

The use of the TEV tool [9] confirms the selection of the COC and t = 4320 s as the most severe thermo-elastic conditions. Fig. 9 illustrates a significant change in the M2 de-center in response to variations in an asymmetric local thermal gradient at the outer part of the central baffle.

Finally, it was determined that the worst thermo-elastic scenario occurs during the science pointing after leaving an eclipse (Fig. 10). In this scenario, the combination of factors includes the telescope being oriented towards the Earth, observing the poles, with the sun impacting obliquely on the baffle, and performing science. This results in significant energy dissipation on the rear side of the vertical optical bench, about 15 W, compared to the Earth's radiation. This leads to local thermal gradients on the baffle itself, as well as along the horizontal and vertical optical benches. This generates, as shown in Fig. 11, local thermal gradients on the baffle itself, as well as along the horizontal and vertical optical benches.

In Fig. 12 there is a comparison between the temperature field on the

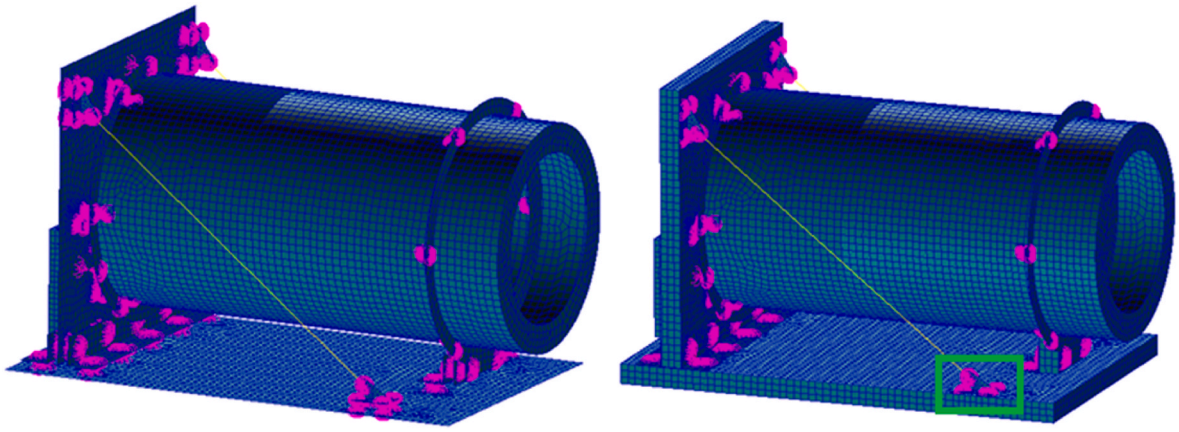

Fig. 7. VINIS's FEM in NASTRAN, with 2D (left) and 3D (right) representation of the sandwich panels, indicating in green the component which was modified to differentiate between "Configuration B" and "Configuration C". (For interpretation of the references to colour in this figure legend, the reader is referred to the Web version of this article.)

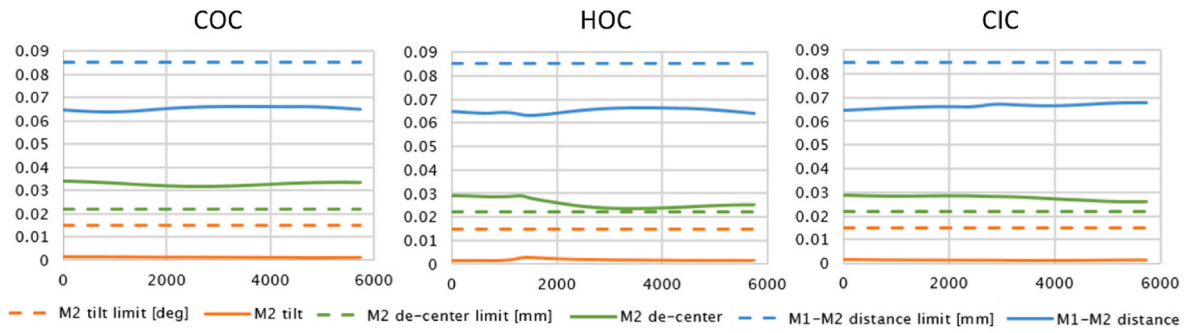

Fig. 8. Performance parameter evolution along the orbit for COC, HOC and CIC scenarios.

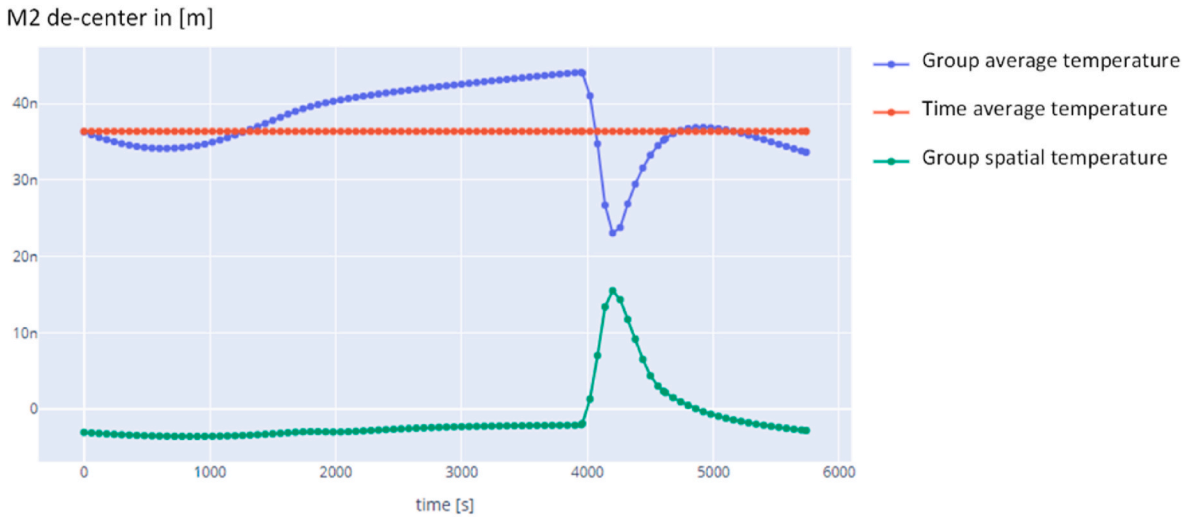

Fig. 9. M2 de-center response to the variation of thermal nodes temperature corresponding to an asymmetric local thermal gradient located the central baffle, using the TEV tool [9].

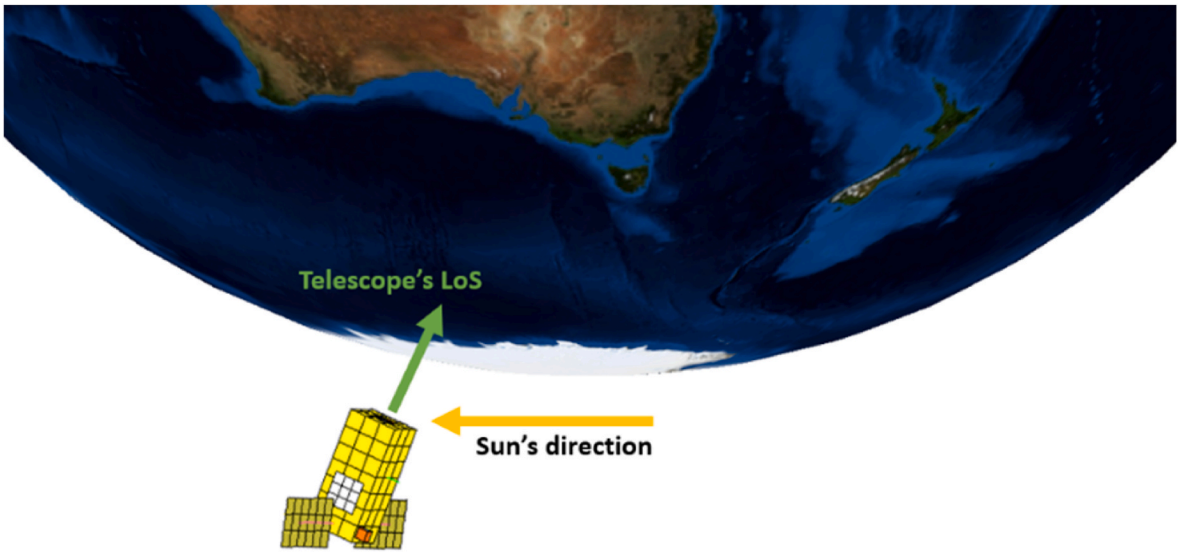

Fig. 10. Diagram of the most demanding thermo-elastic scenario.

thermal and structural numerical models, after performing the temperature mapping. According to this figure, the temperature mapping appears to be accurate and representative of the problem.

With respect to "Configuration C″, after careful adjustment of $k_{j-sh,HOR-OB\ to\ ROD}$, the value of the calibrated spring was set to $2{\cdot}10^5$ N/m. This becomes then the nominal value for performing the uncertainty analysis of "Configuration C".

The evaluation of the uncertainty results will proceed in two steps. Firstly, by assessing the overall uncertainty associated to each performance parameter and determining if it fulfils the design limit values.

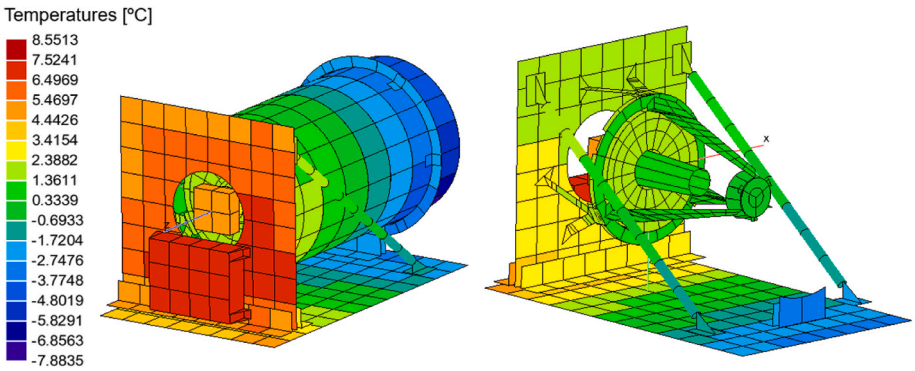

Fig. 11. Telescope temperatures during the worst thermo-elastic scenario (t = 4320 s).

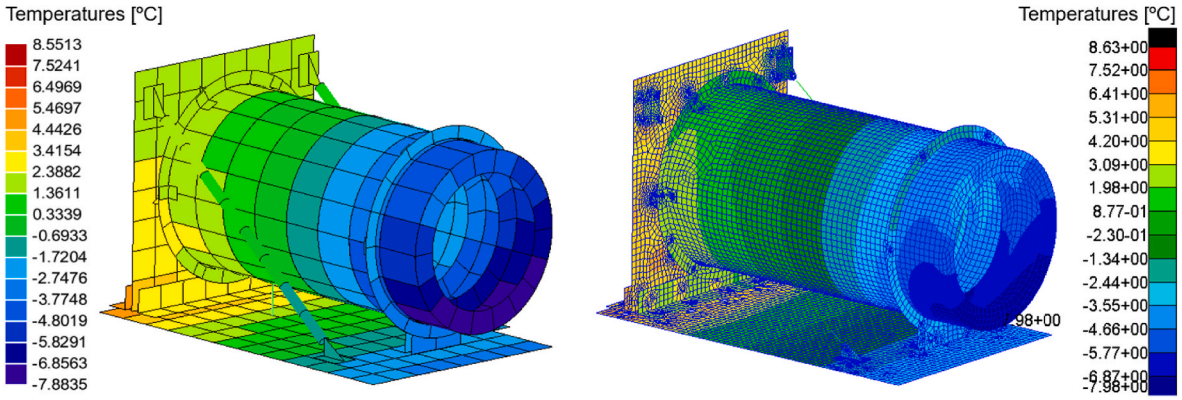

Fig. 12. Temperature mapping results, on the thermal (left) and structural (right) models.

Secondly, by evaluating the contribution of the uncertainty in each input parameter to the overall performance parameter's uncertainty.

To assist in identifying the Thermo-Elastic Deformation Modes (TEDM), Fig. 13 presents the displacement profiles of the complete telescope assembly across the three configurations, under the worst thermo-elastic scenario conditions. These visualizations highlight that the vertical optical bench, along with the central baffle and electronic box, are the components that contribute most to the displacements in the space telescope assembly.

5.2. Global uncertainty assessment

Results from the global uncertainty assessment are gathered in Table 3, Table 4, and Table 5. The outputs from both "Configuration A″ and "Configuration B″ show similar trends, with difficulties in achieving the M2 de-center performance and a narrow margin in the M1-M2 distance when adding the associated global uncertainty. Conversely, the M2 tilt comfortably meets requirements with a wide margin and minimal uncertainty, suggesting this parameter is unlikely to pose any issues for VINIS performance. However, results from "Configuration C″ differ significantly from the rest. After adjusting the response to meet the nominal values, once the uncertainty is added, both the M2 de-center and M1-M2 distance performance parameter fall outside the allowable limits.

5.3. Disaggregated uncertainty assessment

The second phase of the uncertainty assessment focuses on evaluating the individual parameter influence to the overall uncertainty. This detailed analysis, covering all three performance parameters and configurations, aims to identify the parameters which most influence the performance. It also assesses the effects of changes in the sandwich panel formulation or FEM definition.

When analysing these results, it is important to recognize that if the global uncertainty is very low, the contribution of individual input parameters is correspondingly small. In such cases, minor deviations in the assigned uncertainty can significantly alter the results. This is particularly evident in the case of the M2 tilt performance parameter, where both its absolute uncertainty (consistently below 0.0004 mm) and its percentage of the performance requirement (less than 2.6%) are very low. Consequently, the disaggregated results for the M2 tilt parameter are not considered among the ones which dominate the uncertainty of the thermo-elastic response.

From the 148 parameters assessed, only 13 contribute significantly to the total uncertainty in any section of the telescope and its assembly, as summarized in Table 6. These findings highlight that the thermo-elastic response is predominantly driven by structural concerns and one thermal parameter, the Earth's infrared radiation intensity, J_P. The J_P parameter notably impacts performance, aligning with the fact that the telescope, being an Earth observation instrument with direct exposure to Earth's radiation, is greatly affected by its pointing attitude and the variability of Earth's infrared emissivity is large depending on the features to be observed. However, it should be pointed out that it is a parameter that cannot be controlled, as observing Earth is the purpose of the mission. The designer should live with this uncertainty and focus uncertainty reduction and/or redesign efforts on other features.

Referring to Fig. 14, Fig. 15, Fig. 16, it is evident that, among the *controllable* parameters (excluding J_P), the M2 de-center uncertainty in the response is predominantly influenced by stiffness-related factors. The heat dissipation at the BEE causes notable deformations in the vertical optical bench, as $CTE_{Al6061T6}$ and $k_{j-be,OB-VER\ to\ ELEC-BOX}$ are large contributors to the M2 de-center response. Additionally, longitudinal and asymmetric thermal gradients on the central baffle (seen in Fig. 12) contribute to significant deformations through E_{CFRP}, CTE_{CFRP} and

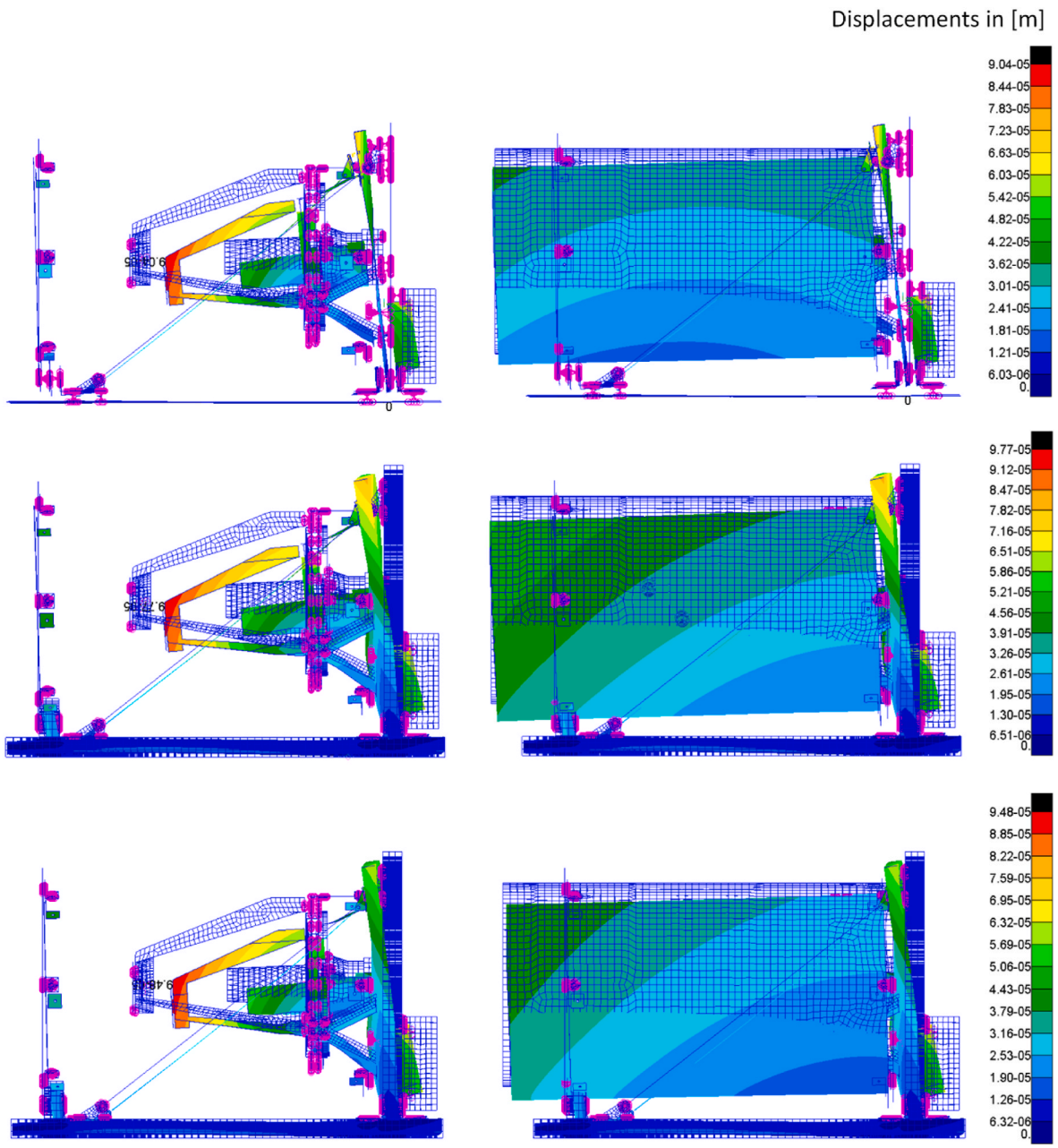

Fig. 13. Displacements for "Configuration A" (top), "Configuration B" (middle) and "Configuration C" (down).

Table 3
Global uncertainty results applied to "Configuration A".

Performance Parameter	Requirement	Nominal result	Uncertainty (2σ)	Nominal result + uncertainty	Uncertainty (% requirement)
M2 tilt [deg]	±0.015	0.0005	0.0003	0.0008	2.0
M2 de-center [mm]	±0.022	0.0372	0.0074	0.0446	33.6
M1-M2 distance [mm]	±0.085	−0.0615	0.0118	−0.0733	13.9

Table 4
Global uncertainty results applied to "Configuration B".

Performance Parameter	Requirement	Nominal result	Uncertainty (2σ)	Nominal result + uncertainty	Uncertainty (% requirement)
M2 tilt [deg]	±0.015	0.0016	0.0004	0.0020	2.7
M2 de-center [mm]	±0.022	0.0330	0.0080	0.0410	36.4
M1-M2 distance [mm]	±0.085	−0.0659	0.0117	−0.0776	13.8

Table 5
Global uncertainty analysis applied to "Configuration C".

Performance Parameter	Requirement	Nominal result	Uncertainty (2σ)	Nominal result + uncertainty	Uncertainty (% requirement)
M2 tilt [deg]	±0.015	0.0022	0.0004	0.0026	2.7
M2 de-center [mm]	±0.022	0.0204	0.0069	0.0273	31.4
M1-M2 distance [mm]	±0.085	−0.0821	0.0127	−0.0949	14.9

Table 6
Principal contributors to thermo-elastic uncertainty (see Fig. 1 for acronyms).

Input Parameter (IP)	Symbol	Type	Description
Earth IR radiation intensity	J_P	TR	Radiative parameter which reflects the Earth's IR radiation intensity, a source of uncertainty inherent to the operation of an Earth observation telescope. The telescope's aperture significantly determines its thermal behaviour.
Young Modulus	E_{CFRP}	S	CFRP Young Modulus, predominantly used as the CEN-BAF material.
CTE	$CTE_{Al6061T6}$	S	Al6061T6 CTE, material employed for the ELEC-BOX, a component which significant dissipation during science operation.
CTE	CTE_{AlSi40}	S	AlSi40 CTE. This material conforms the complete telescope assembly, including M1, M1-SUP, SPID, M2, INN-BAF and FPA-SUP.
CTE	CTE_{CFRP}	S	CFRP CTE, employed on the CEN-BAF.
CTE	$CTE_{Ti6Al4V}$	S	Ti6Al4V CTE, material applied to BIP, the components in charge of disaggregate the translation of deformations from the vertical optical bench to the telescope train.
Joint axial stiffness	$k_{j-ax,OB-VER\ to\ CEN-BAF}$	S	Joint axial stiffness between OB-VER and CEN-BAF.
Joint bending stiffness	$k_{j-be,OB-VER\ to\ ELEC-BOX}$	S	Joint bending stiffness between OB-VER and ELEC-BOX.
Joint shear stiffness (spring constant)	$k_{j-sh,OB-HOR\ to\ OB-ROD}$	S	Joint shear stiffness between OB-HOR and OB-ROD. Parameter relevant just for "Configuration C″, as it is the structural property which has been modified with respect to "Configuration B″ to adjust the nominal response.
Joint shear stiffness	$k_{j-sh,OB-VER\ to\ CEN-BAF}$	S	Joint shear stiffness between OB-VER and CEN-BAF.
Joint shear stiffness	$k_{j-sh,OB-VER\ to\ ELEC-BOX}$	S	Joint shear stiffness between OB-VER and ELEC-BOX.
Sandwich in-plane stiffness	$k_{s-ip,OB-VER}$	S	Sandwich in-plane stiffness of the OB-VER.
Sandwich bending stiffness	$k_{s-be,OB-VER}$	S	Sandwich bending stiffness of the OB-VER.

$k_{j-sh,OB-VER\ to\ CEN-BAF}$ elements. These factors lead to considerable bending in the vertical optical bench, indicated by $k_{s-ip,OB-VER}$ and $k_{s-be,OB-VER}$. In "Configuration C″, the impact of $k_{j-sh,OB-HOR\ to\ OB-ROD}$ on performance is more pronounced due to the changes in the FEM definition, relegating J_P parameter to the third place.

Analysing the uncertainty in the M1-M2 distance from the results in Fig. 17, Figs. 18 and 19, it becomes clear that in this case the response is largely governed by CTE effects, with CTE_{AlSi40} as the primary contributor. This is a direct consequence of the telescope's design, where the telescope train is entirely composed of high conductive AlSi40 material, thereby minimizing thermal gradients within the structure. Therefore, the primary deformation mechanism affecting the distance between the two mirrors arises from the expansion or contraction of the material in the spider structure. Again, in "Configuration C″, the parameter $k_{j-sh,OB-HOR\ to\ OB-ROD}$ also plays a significant role in the response.

6. Discussion

The main outcome of this research is that an uncertainty analysis methodology to assess the performance of a space telescope have been successfully integrated. This is relevant since, while uncertainty analysis and thermo-elastic analysis are well-established tools individually, their combined application presents a novel approach. It is important to note that the primary goal of these thermal and structural models is not to precisely simulate behaviour to the highest degree of fidelity, but rather to develop a parametric model that is precise enough for its end and that facilitates the determination of each element's relevance through uncertainty analysis. This method proved to be effective in identifying the specific elements with the highest potential to cause significant thermo-elastic deformations, setting a method to share results between analysis with different mathematical bases.

Having followed ESA's TEV guidelines gives a very good understanding of the main TEDM in the design. These features include local thermal loads on the front part of the central baffle and the assembly of the electronics box on the same optical bench where the telescope is mounted. The authors of this paper find that this process is a very necessary first step to understand the overall physical behaviour and mechanisms implied. However, performing this uncertainty analysis is key in identifying the specific thermo-elastic parameters and factors, in the early design phase, that drive those mechanisms that might risk the mission's success. In this way the specific main actionable parameters, mainly sandwich panel and joints stiffnesses, were identified. Also, a thermal parameter which cannot be acted upon, the Earth's infrared radiation intensity, was identified and the fact that there is some part of uncertainty that will be present during all the design process was acknowledged.

It was not possible to find a solution that completely satisfies the performance parameters by solely modifying the numerical model parameters. As seen in "Configuration C″, the nominal solution lies within specifications, but once margins are added, they exceed the established limits. There could be two ways forward here: either the solution could be taken as good, as uncertainty would expect to be reduced in the future with testing or a more in-depth redesign might be attempted. Observing the uncertainty results it can be seen that the high sensitivity of the results to the modified parameter indicates that the first option might not be advisable. Even if the spring is carefully calibrated the element under tension might vary its stiffness during the mission's life. On top, there is some permanent uncertainty that cannot be reduced, and this design is quite close to its operational limits. Therefore, design modifications, not just numerical model adjustments, are necessary to robustly meet the performance requirements. Furthermore, any proposed solution should ensure a robust response not from a thermo-elastic perspective, but also from a structural standpoint. To achieve this, the engineers responsible for the VINIS telescope design can refer to the uncertainty analysis results to identify the mechanisms that dominate

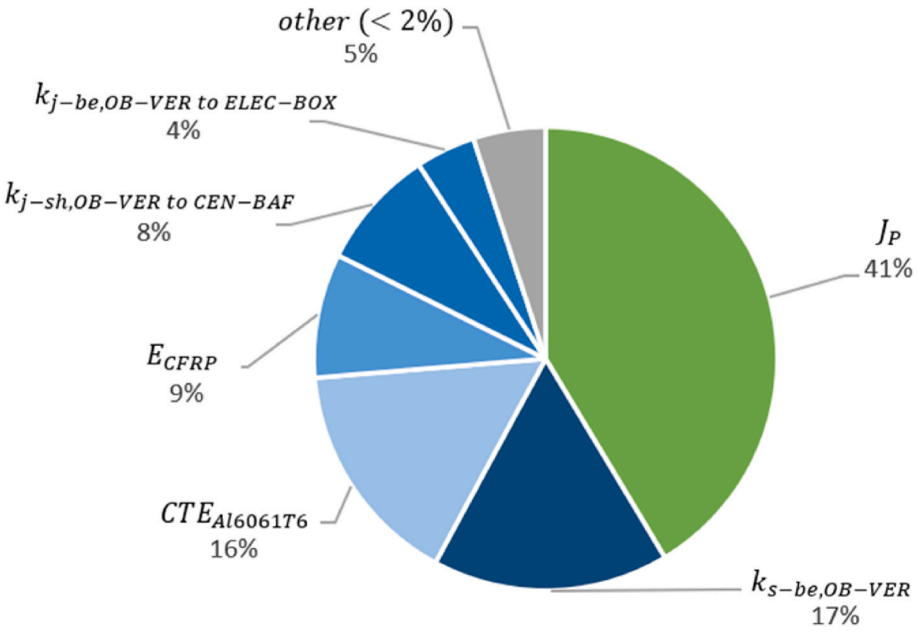

Fig. 14. Main contributors to the uncertainty in the response of the **M2 de-center** performance parameter for "**Configuration A**″, 2σ global uncertainty: 0.0074. "TR" parameters in green, "S" in blue, and others in grey. The full pie is 100% of w_{P_i}. See Fig. 1 for acronyms. (For interpretation of the references to colour in this figure legend, the reader is referred to the Web version of this article.)

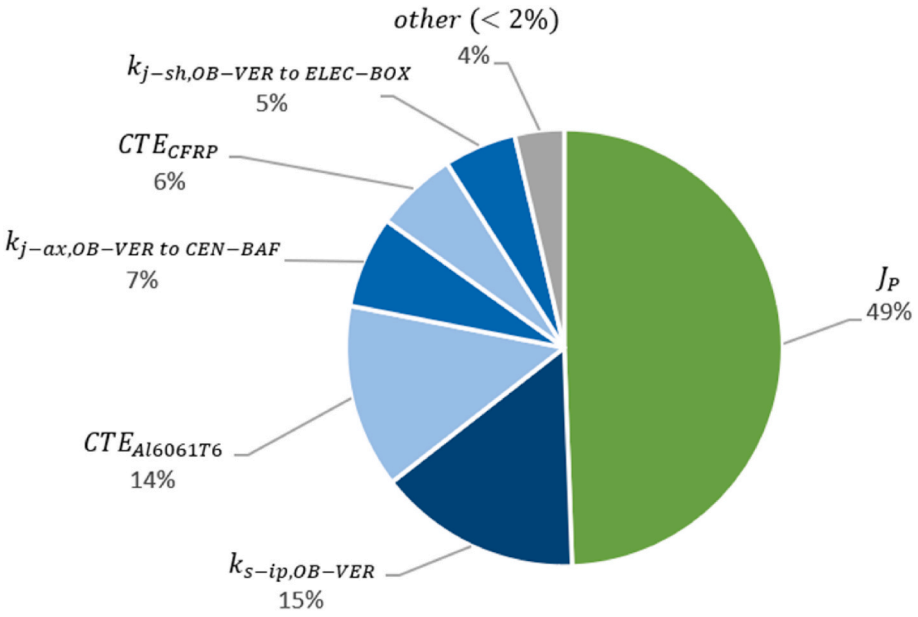

Fig. 15. Main contributors to the uncertainty in the response of the **M2 de-center** performance parameter for "**Configuration B**″, 2σ global uncertainty: 0.0080. "TR" parameters in green, "S" in blue, and others in grey. The full pie is 100% of w_{P_i}. See Fig. 1 for acronyms. (For interpretation of the references to colour in this figure legend, the reader is referred to the Web version of this article.)

the uncertainty in the thermo-elastic response and seek to minimize them. The results of the uncertainty analysis show that the vertical sandwich panel's stiffness parameters are the main driver parameters that can be acted upon, thus design actions relieving that panel are a promising way forward. One possible solution will be to re-locate the electronic box which lies attached to the vertical optical bench and detach the baffle from the vertical panel and attach it to the horizontal panel (checking dynamic response results as well).

Uncertainty analysis is a complex subject so there are several attention points to consider. It is important to cautiously interpret the results of the uncertainty analysis, viewing them more as a qualitative measure of the dominant TEDM in the response rather than as an exact quantification of each one's contribution to the overall uncertainty. One important factor to consider here is that knowing precisely the uncertainty associated to a parameter is an almost impossible task. It might be known if it's high (let's say 30%–50%) or low (3%–5%), but the exact number will be unknown. This will make that the rank of influencing parameters might vary from one consideration to another, but the important parameters will be present in both configurations.

In this regard also, for example one might expect that the overall uncertainty results for the 3D configuration of the panels are lower than for the 2D equivalent model, when they appear to be slightly higher,

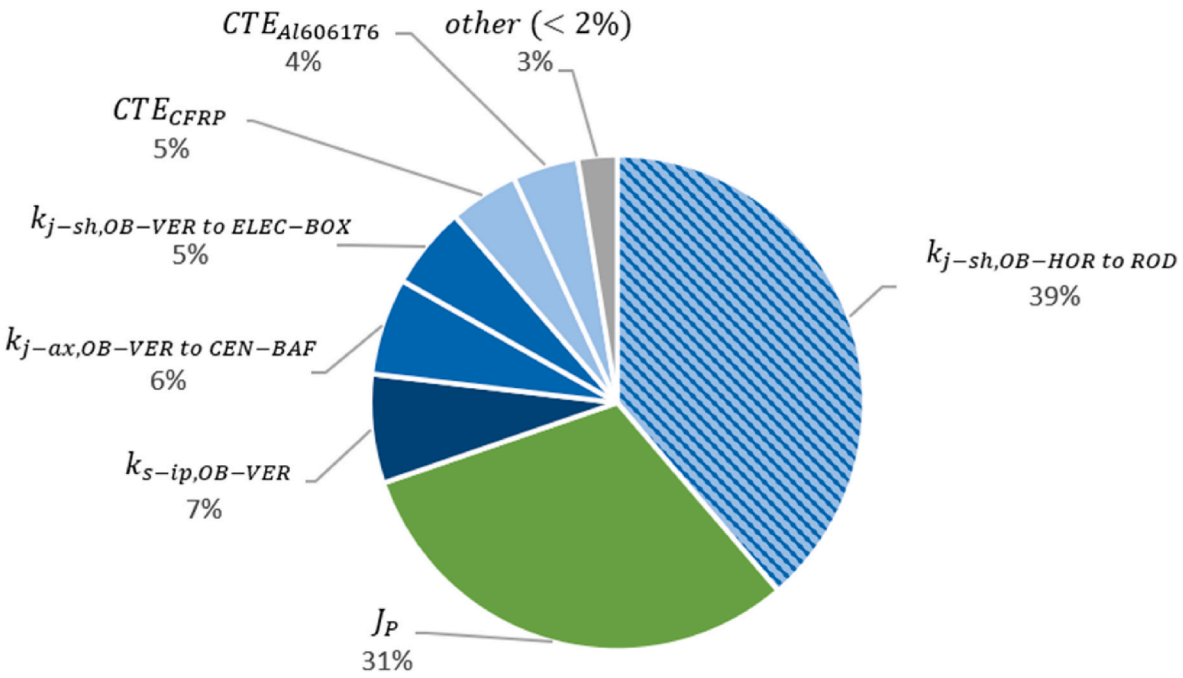

Fig. 16. Main contributors to the uncertainty in the response of the **M2 de-center** performance parameter for "**Configuration C**″, 2σ global uncertainty: 0.0069, with the parameter modified with respect to "B" with striped background. "TR" parameters in green, "S" in blue, and others in grey. The full pie is 100% of w_{P_i}. See Fig. 1 for acronyms. (For interpretation of the references to colour in this figure legend, the reader is referred to the Web version of this article.)

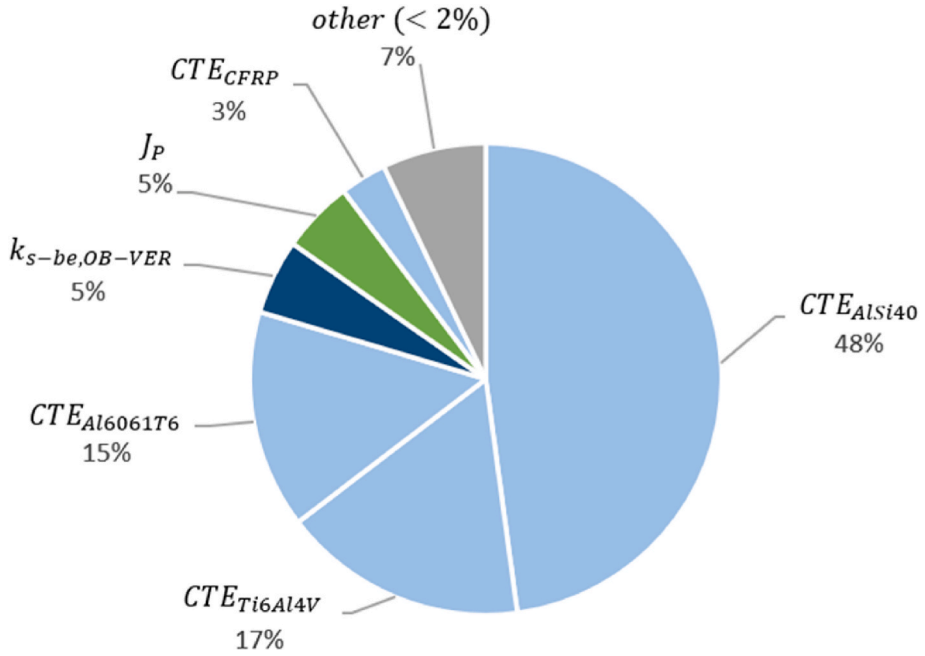

Fig. 17. Main contributors to the uncertainty in the response of the **M1-M2 distance** performance parameter for "**Configuration A**″, 2σ global uncertainty: 0.0118. "TR" parameters in green, "S" in blue, and others in grey. The full pie is 100% of w_{P_i}. See Fig. 1 for acronyms. (For interpretation of the references to colour in this figure legend, the reader is referred to the Web version of this article.)

even with a larger initial uncertainty of the 2D properties. Well, in the 3D configuration the sensitivity is slightly larger, large enough to compensate the decrease in uncertainty parameter (it should be recalled that the uncertainty is the product of sensitivity times uncertainty of the parameter). The main conclusion here is that these parameters in the end are some of the main drivers of the response and should be a key element when designing future tests for adjusting the models.

Similarly, caution is needed when interpreting the results of disaggregated uncertainty, especially if the global uncertainty associated with a specific parameter is very small. In such cases, if the global uncertainty is significantly smaller than the design limits (as with the M2 tilt, always below 2.6%), the dominating TEDMs in that response can be considered negligible in terms of design risk. Conversely, if there is a very small associated uncertainty that falls outside the design limits, the team responsible for the thermo-elastic design should consider making modifications to the design itself, as it is highly unlikely that deviations

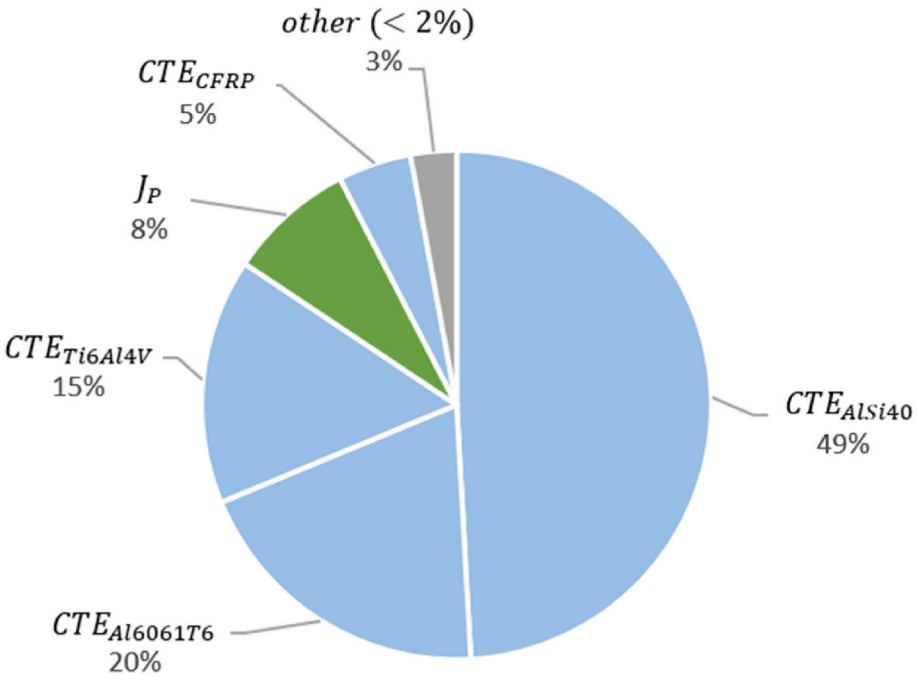

Fig. 18. Main contributors to the uncertainty in the response of the **M1-M2 distance** performance parameter for "**Configuration B**″, 2σ global uncertainty: 0.0117. "TR" parameters in green, "S" in blue, and others in grey. The full pie is 100% of w_{P_i}. See Fig. 1 for acronyms. (For interpretation of the references to colour in this figure legend, the reader is referred to the Web version of this article.)

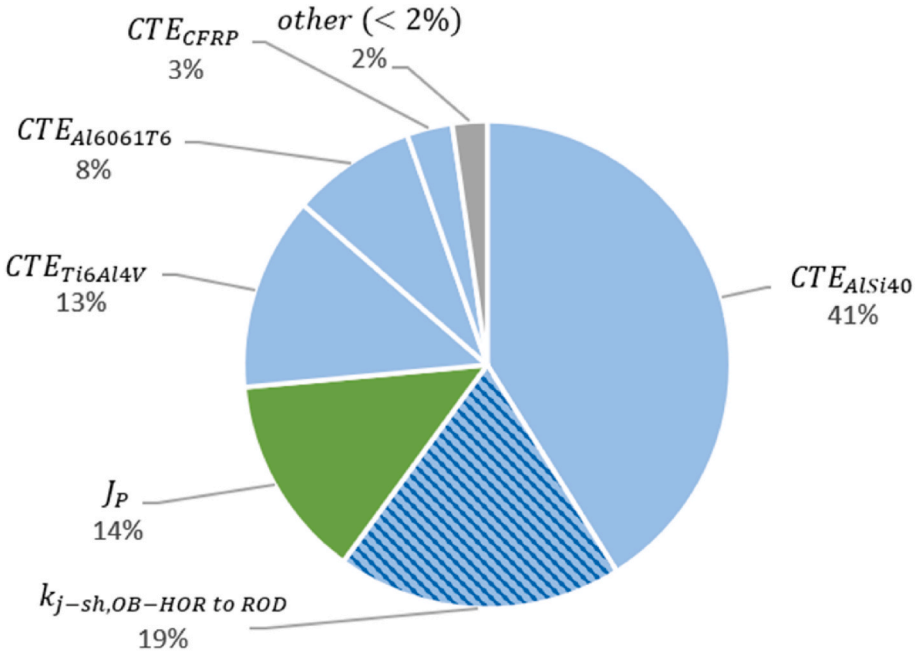

Fig. 19. Main contributors to the uncertainty in the response of the **M1-M2 distance** performance parameter for "**Configuration C**″, 2σ global uncertainty: 0.0127, with the parameter modified with respect to "B" with striped background. "TR" parameters in green, "S" in blue, and others in grey. The full pie is 100% of w_{P_i}. See Fig. 1 for acronyms. (For interpretation of the references to colour in this figure legend, the reader is referred to the Web version of this article.)

can be corrected through numerical model adjustments alone.

There is one more point of attention to be considered. Uncertainty results depend on both uncertainty of input parameters and sensitivity to these parameters. Therefore, if the variation of a performance parameter with respect to an input parameter is null the associated uncertainty will be null to. This might be the case for irrelevant parameters, but it might also happen for parameters which are out of their sensitive zone. For example, they are too stiff so a variation in that stiffness region will not produce changes, but connections in that area are an important part of the response. This happened with results from "Configuration C". The stiffness in that connection was too high to drive the response but reducing it took it to a point where there was a high associated uncertainty. For this reason, it is important to keep in mind that, even if the uncertainty analysis is a very powerful tool to analyse thermo-elastic behaviour it is important to use it in combination with an analytical process such as the one proposed in the TEV guidelines because

understanding physical behaviour is essential.

So, as a final word, uncertainty analysis as a tool for assessing thermo-elastic performance and design has been tested and found to be a very powerful tool for driving design of optical telescopes. It has also been made evident, that there are some caution points to be considered. Also, the procedure in ESA's TEV guidelines has been put to a test and has been found very useful in understanding the underlying physical behaviour. Although both methodologies have their strong and weak points the authors of this paper have reached the conclusion that, combining both methods will give both a good understanding of the main TEDM and a powerful analytical way of identifying which specific parameters drive those TEDM. In fact, the use of this uncertainty approach can multiply the understanding given by the TEV approach and the TEV might provide insight to put into context the results given by the uncertainty analysis. If only one of the methods should be used, the authors believe that uncertainty analysis might give the best overall result, as it provides understanding through analytical results, but the combination of both will give the best results for improving the design process of any device in which thermo-elastic effect are of concern.

Future lines

When evaluating future research directions, the foremost idea is to broaden the methodology across the full STOP analysis chain. This extension aims to provide more comprehensive insights into affected optical parameters, thereby enabling more accurate adjustments. Consequently, the performance metric would transition from relying on structural analysis results to optical outputs.

Another topic for further insight is the TEV set of tools. It was released halfway through the work shown in this paper and it could only be used superficially, but it shows great potential for example for assisting in the determination of the most critical cases, so its use should be further explored in the future.

Additionally, there exists the potential to follow the approach from Ref. [49], and employ multifid approaches, GSA or even multifid estimators, to compute the global sensitivity employing stochastic methods while decreasing the computational time of the analysis. In this context, a comparative analysis of the results could be conducted, assessing whether the increase in complexity is justified by more accurate results.

Declaration of generative AI and AI-assisted technologies in the writing process

During the preparation of this work the authors used Chat GPT 4.0 in order to improve readability and language. After using this tool/service, the authors reviewed and edited the content as needed and take full responsibility for the content of the publication.

Declaration of competing interest

The authors declare that they have no known competing financial interests or personal relationships that could have appeared to influence the work reported in this paper.

Acknowledgements

This research was funded by MCIN/AEI/10.13039/501100011033, grant number PID2022-141669OA-I00. This research was conducted with the support of a doctoral grant awarded to Uxia Garcia-Luis under the "Programa de axudas á etapa predoutoral da Xunta de Galicia" by the Galician Regional Government (Consellería de Cultura, Educación, Formación Profesional e Universidades). The authors wish to extend their gratitude to the Cabildo de Canarias for the financial support that facilitated the research contracts for some members at IACTEC-Espacio, as well as allowing the use of their space telescope's preliminary design. This contribution has been instrumental in assessing the innovative thermo-elastic methodology, further enriching the practical application of the research. Funding for open access charge: Universidade de Vigo/CISUG.

References

[1] G. Cottrell, Telescopes: A Very Short Introduction, Oxford University Press, 2017. ISBN: 0198745869.
[2] P.A. Oche, E. Gideon Ata, N. Ibekwe, Applications and challenges of artificial intelligence in space missions, IEEE Access (2021), https://doi.org/10.1109/ACCESS.2021.3132500.
[3] J. Kua, W.L. Seng, A. Chetan, F. Niroshinie, R. Chathurika, Internet of things in space: a review of opportunities and challenges from satellite-aided computing to digitally-enhanced space living, Sensors 21 (2021), https://doi.org/10.3390/s21238117.
[4] V.S. Chippalkatti, S.S. Rana, R.C. Biradar, Big paradigm shift in small satellite technology and applications, Advances in Small Satellite Technologies (2023), https://doi.org/10.1007/978-981-19-7474-8_22.
[5] E.S. Douglas, K. Tracy, Z. Manchester, Practical limits on nanosatellite telescope pointing: the impact of disturbances and photon noise, Astronomical Instrumentation 8 (2021), https://doi.org/10.3389/fspas.2021.676252.
[6] L. Li, Y. Yu, L. Wang, L. Yuan, L. Zhang, X. Gong, Y. Wu, R. Zheng, Modeling and analysis of the influence caused by micro-vibration on satellite attitude control system, Acta Astronaut. 213 (2023) 71–80, https://doi.org/10.1016/j.actaastro.2023.08.047.
[7] S. Appel, J. Wijker, Simulation of Thermoelastic Behaviour of Spacecraft Structures, Springer, Noordwijk, The Netherlands, 2021, https://doi.org/10.1007/978-3-030-78999-2.
[8] B. Putz, S. Wurster, T.E.J. Edwards, B. Völker, G. Milassin, D.M. Többens, C.O. A. Semprimoschnig, M.J. Cordill, Mechanical and optical degradation of flexible optical solar reflectors during simulated low earth orbit thermal cycling, Acta Astronaut. 175 (2020) 277–289, https://doi.org/10.1016/j.actaastro.2020.05.032.
[9] Esa/Estec Tec-M, European Guidelines for Thermo-Elastic Verification, first ed., Noordwijk, The Netherlands, 2023. STM-285.
[10] A. Gonzalez-Llana, A. Van Oostrum, A. Peman, M. De Cillia, S. Rapp, M. Meschenmoser, V. Mareschi, S. De Palo, L. Perachino, S. Appel, Practical Example of a Thermo-Elastic Classification System, ECSSMET, Toulouse, France, 2023.
[11] L. Perachino, B. Laine, S. De Palo, V. Mareschi, F. Acquaviva, J. D'Amico, S. Behar-Lafenetre, P. Baussart, S. Appel, M. Vaughan, S. Sablerolle, H. Ertel, M. De Cilla, P. Atinsounon, Improvement of Methodologies for Thermo-Elastic Predictions and Verification, ECSSMET, Virtual Event, 2021.
[12] A. García-Pérez, G. Alonso, A. Gómez-San-Juan, J. Pérez-Álvarez, Thermoelastic evaluation of the payload module of the ARIEL mission, Exp. Astron. 53 (2021) 831–846, https://doi.org/10.1007/s10686-021-09704-0.
[13] A. Gómez-San-Juan, Análisis de incertidumbres en sistemas de control térmico en ambientes espaciales, ETSIAE, Universidad Politécnica de Madrid, Madrid, Spain, 2018.
[14] M. Salgado-Rodriguez, U. Garcia-Luis, A. Gomez-San-Juan, C. Ulloa-Sande, F. Navarro-Medina, Conceptual design and research on the thermal performance of a martian human base, Acta Astronaut. (2022) 524–538, https://doi.org/10.1016/j.actaastro.2022.08.010.
[15] U. Garcia-Luis, A. Gomez-San-Juan, F. Navarro-Medina, A. Aguado-Agelet, C. Ulloa-Sande, G. Rey-Gonzalez, P. Orgeira-Crespo, A. Camanzo-Mariño, V. Dragos-Darau, A.E. Pelaez-Santos, P. Gonzalez De Chavez Fernandez, A. Ynigo-Rivera, Uncertainty Based Method for Assessing Critical Thermo-Elastic Parameters for Space Telescopes Performance, ECSSMET, Toulouse, France, 2023.
[16] U. Garcia-Luis, Thermo-elastic Study of the Pointing Platform for Space Telescopes, University of Vigo, 2023.
[17] S.R. Blattnig, L.L. Green, J.M. Luckring, J.H. Morrison, R. Tripathi, T.A. Zang, Towards a credibility assessment of models and simulations, in: 49th AIAA/ASME/ASCE/AHS/ASC Structures, Structural Dynamics, and Materials, Schaumburg, US, 2008.
[18] A. Saltelli, K. Chan, E.M. Scott, Sensitivity Analysis, John Wiley & Sons, New York, 2000. ISBN: 978-0-470-74382-9.
[19] W. Ousley, Requirements for Thermal Design, Analysis and Development. 545-PG-8700.2.1A, NASA Thermal Engineering Branch, 2005.
[20] J.W. Welch, Comparison of satellite flight temperatures with thermal Predictions, SAE International 115 (2006) 524–530.
[21] ESA-ESTEC Requirements & Standards Division, "ECSS Standards, Space Engineering - Thermal Control General Requirements, ECSS-E-ST-31C, 2008.
[22] ESA-ESTEC Requirements & Standards Division, "ECSS Standards, Structural General Requirements - ECSS-E-ST-32c, 2008.
[23] ESA-ESTEC Requirements & Standards Division, "ECSS Standards, Structural Factors of Safety for Spaceflight Hardware - ECSS-E-ST-32-10c, 2009.
[24] S.J. Kline, F.A. McClintock, Describing uncertainties in single-sample experiments, ASME Mechanical Engineering 75 (1953) 3–8.
[25] ESA-ESTEC Requirements & Standards Division, "ECSS Standards, Space Engineering - Testing, ECSS-E-ST-10-03C, 2002.
[26] ESA-ESTEC Requirements & Standards Division, ECSS Standards: Space Engineering - Testing, ECSS-E-10-03A, 2012.
[27] ESA-ESTEC Requirements & Standards Division, ECSS-E-HB-31-03A: Thermal Analysis Handbook, 2016.

[28] D.P. Thunnissen, S.K. Au, G.T. Tsuyuki, Uncertainty quantification in estimating critical spacecraft component temperatures, J. Thermophys. Heat Tran. 1 (2007) 422–430, https://doi.org/10.2514/1.23979.
[29] K. Dale Stout, Bayesian-based Simulation Model Validation for Spacecraft Thermal Systems, PhD Thesis, Massachusetts Institute of Technology, 2015.
[30] Blue Engineering - Stochastic Team, Guidelines for the Assesment and Implementation of Stochastic Methods for Space Thermal Analysis, Technical report: 02.07.035/TN5, Blue Engineering, 2004.
[31] D. Ballhause, W. Konrad, Stochastic Analysis of Dimensional Stability of Instrument Structures, ECSSMET, Noordwijk, The Netherlands, 2012.
[32] S. Appel, A. Peman, Quantifying Uncertainties in Thermoelastic Predictions, ECSSMET, Noorwijk, The Netherlands, 2021.
[33] M. Padulo, M.S. Campobasso, M.D. Guenov, Novel uncertainty propagation method for robust aerodynamic design, AIAA J. 49 (2011) 530–543, https://doi.org/10.2514/1.J050448.
[34] J. Brynjarsdóttir, A. Kennedy, Learning about physical parameters: the importance of model discrepancy, Inverse Probl. 30 (2014), https://doi.org/10.1088/0266-5611/30/11/114007.
[35] E.R. Canavan, J.G. Tuttle, Thermal conductivity and specific heat measurements of candidate structural materials for the JWST optical bench, AIP Conf. Proc. 824 (1) (2006) 233–240, https://doi.org/10.1063/1.2192356.
[36] J. Tuttle, E. Canavan, Recent NASA/GSFC cryogenic measurements of the total hemispheric emissivity of black surface preparations, IOP Conf. Ser. Mater. Sci. Eng. 102 (1) (2015), https://doi.org/10.1088/1757-899X/102/1/012015.
[37] T. Ishimoto, J.T. Bevans, Temperature variance in spacecraft thermal analysis, Journal of Spacecraft 5 (11) (1968) 1372–1376, https://doi.org/10.2514/6.1968-62.
[38] R.G. Goble, Temperature uncertainties associated with spacecraft thermal analyses, in: AIAA 6th Thermophysics Conference, Tennesee, US, 1971.
[39] R.K. McGregor, Limitations in thermal scale modeling, Journal of Spacecraft 8 (5) (1971) 559–560, https://doi.org/10.2514/3.30312.
[40] D.J. Zigrang, Comparison of Monte Carlo and statistical treatmetns of heat-transfer data uncertainties, Journal of Spacecraft 14 (9) (1977) 546–549, https://doi.org/10.2514/3.57235.
[41] D. Magrin, V. Viotto, T. Beck, G. Bruno, M. Baroni, A. Turella, M. Marinai, M. Bergomi, A Comparison between the Opto-Thermo-Mechanical Model and Lab Measurements for CHEOPS, SPIE Astronomical Telescopes and Instrumentation, 2018, https://doi.org/10.1117/12.2313406.
[42] J. Junker, G. Bleicher, A. Mottaghibonab, O. Nicolay, C. Reese, M. Appoloni, M. Galdo, D. Teti, PLATO spacecraft: thermo-elastic distortion verification concept and demostration tests, in: *ECSSMET*, Virtual Event, 2021.
[43] ESA, Herschel Observers' Manual, HERSCHEL-HSC-DOC-0876), 2014.
[44] NASA, The Solar Array-Induced Disturbance of the Hubble Space Telescope Pointing System, NASA, Alabama, US, 1995, https://doi.org/10.2514/3.26664.
[45] P.R. Yoder, D. Vukobratovich, Opto-Mechanical Systems Design. Design and Analysis of Opto-Mechanical Assemblies, CRC Press, Taylor & Francis Group, Florida, US, 2015. ISBN: 9781482257700.
[46] K.B. Doyle, V.L. Genberg, G.J. Michels, Integrated Optomechanical Analysis, SPIE—The International Society for Optical Engineeri, Washington, US, 2002, https://doi.org/10.1117/3.974624.
[47] G. De Zanet, A. Viquerat, G. Aglietti, Predicted thermal response of a deployable high-strain composite telescope in low-Earth orbit, Acta Astronaut. 205 (2023) 127–143, https://doi.org/10.1016/j.actaastro.2023.01.034.
[48] G. Dellino, C. Meloni, Uncertainty Management in Simulation-Optimization of Complex Systems, Algorithms and Applications, New York, US: Springer, 2015, https://doi.org/10.1007/978-1-4899-7547-8.
[49] G. Cataldo, E. Qian, J. Auclair, Multifidelity uncertainty quantification and model validation of large-scale multidisciplinary systems, J. Astronomical Telesc. Instrum. Syst. 8 (3) (2022), https://doi.org/10.1117/1.JATIS.8.3.038001.
[50] I.M. Sobol, Sensitivity estimates for nonlinear mathematical models, Mathematical Modelling and Computational Experiments 4 (1993) 407–414.
[51] M. Koot, S. Appel, S. Simonian, Temperature Mapping for Structural Thermoelastic Analysis; Method Benchmarking, ECSSMET, Noordwijk, The Netherlands, 2018.
[52] J.H. Lim, Thermal pointing error analysis of the observation satellites with interpolated temperature based on PAT method, Journal of Korean Society for Aeronaytical and Space Sciences (2015), https://doi.org/10.5139/JKSAS.2016.44.1.80.
[53] A. Baranne, Optical alignment, in: The Construction of Large Telescopes, Tucson, US, 1965.
[54] ESA-ESTEC Requirements & Standards Division, ECSS Standards, Space Engineering - Thermal Analysis Handbook, ECSS-E-HB-31-03A, 2016.
[55] S. Appel, S. Blake, J. Etchells, L. Gambicorti, M. Rieder, T. Bandy, V. Cessa, D. Piazza, End-to-end analysis process on PLATO TOU, in: *ECSSMET*, Virtual Event, 2021.
[56] ESA ESTEC Requirements & Standards Division, "ECSS Standards, Space Engineering, Structural Finite Element Models, ECSS-E-ST-32-03C, Noordwijk, The Netherlands, 2008.